The Cosmic Web

Simulations show that the gravitational contraction of matter from the early universe forms a "cosmic web", with rich clusters at the intersections of filaments.

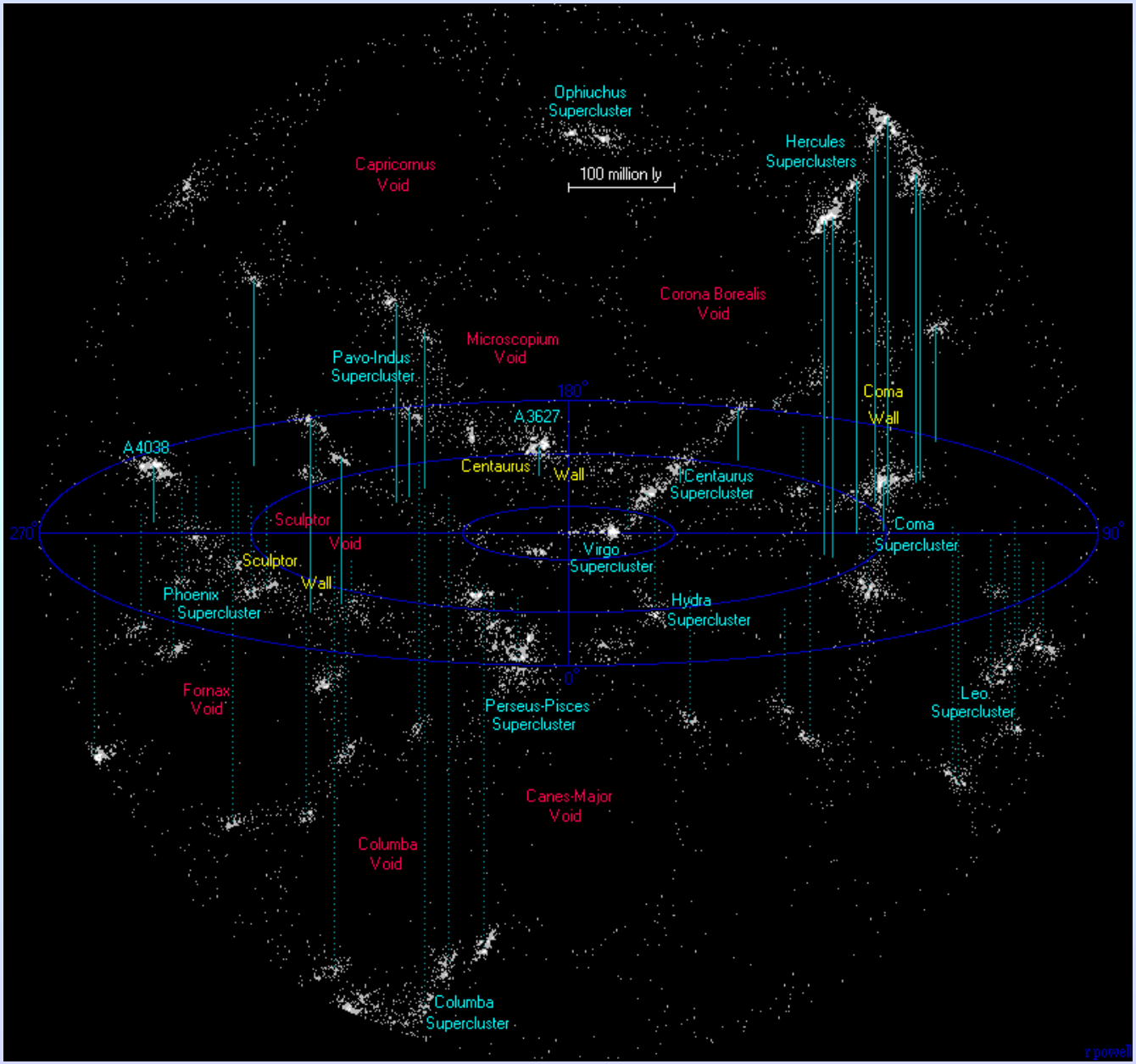

Groups and Clusters

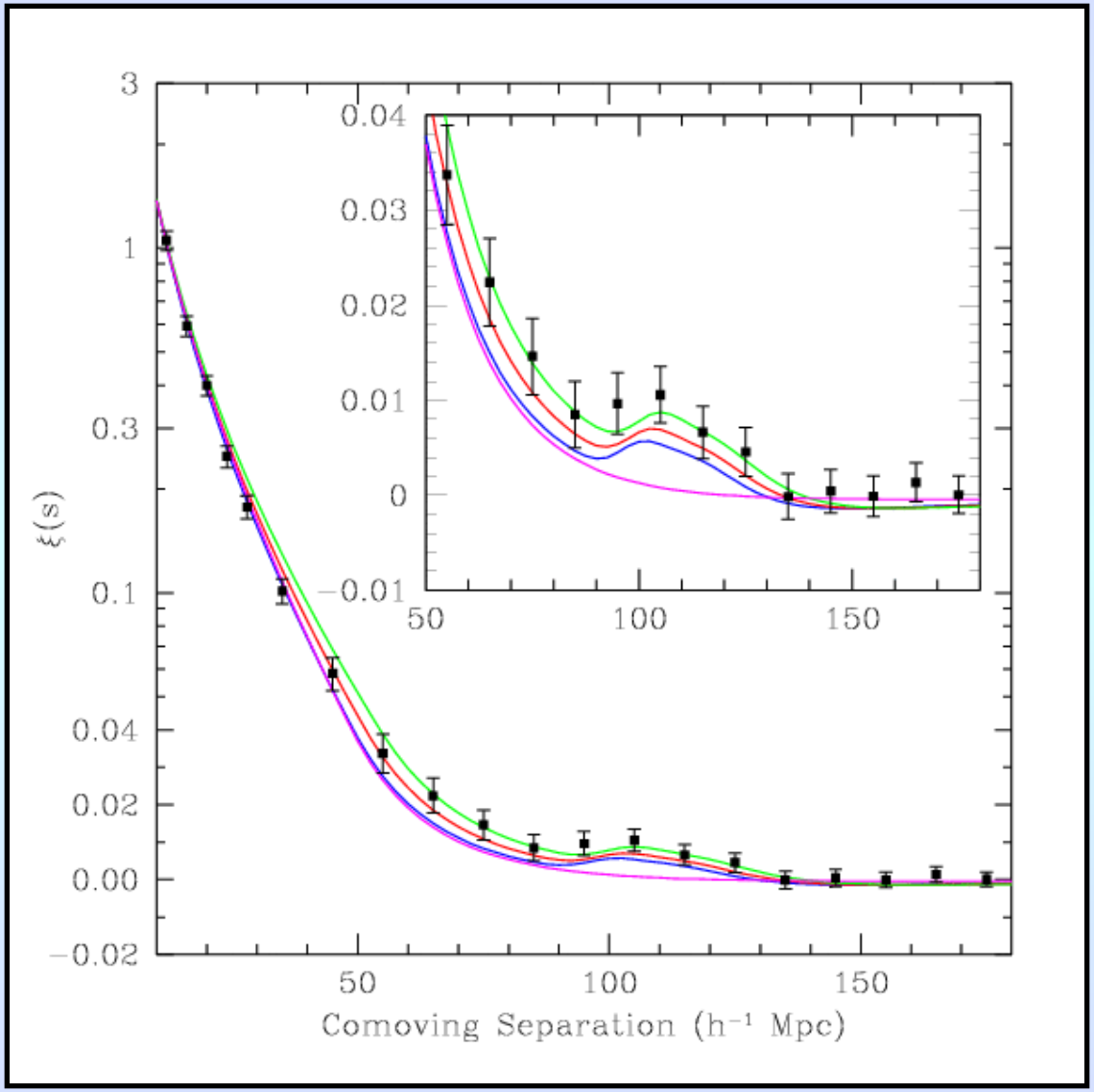

$$dP_{12} = \bar{n}\left\{1 + \xi_{12}(r)\right\} dV_1\, dV_2$$

Galaxy clustering is most often described using the 2-point correlation function, $\xi(r)$, which states how much more likely it is to find a galaxy within a distance r of another galaxy than expected from a random distribution.

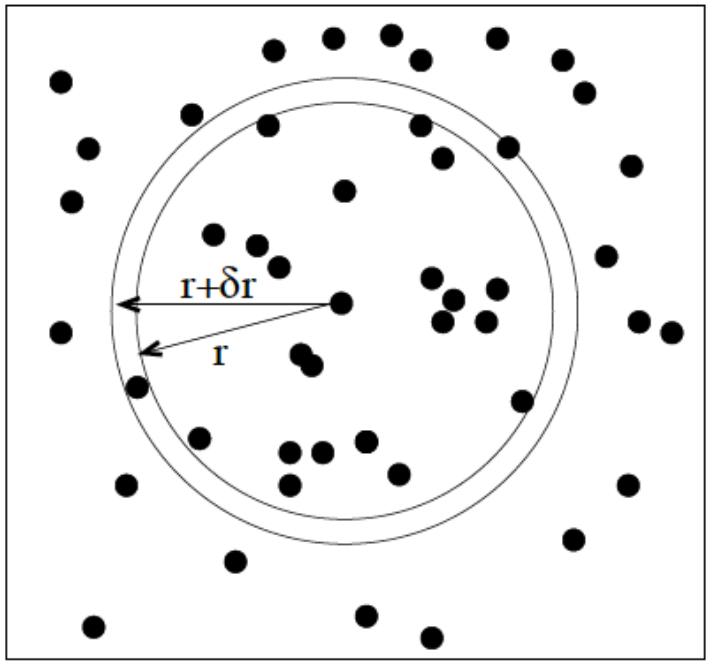

Groups and Clusters

As with most objects in the universe, there are more small galaxy groups than rich clusters. The largest bound structures in the universe are the rich galaxy clusters. These systems have masses of $\sim 10^{15}\ M_{\odot}$.

Simulations demonstrate that the greater the mass of a class of objects, the more highly clustered those objects are. The richest galaxy clusters are highly clustered; low-mass galaxies are almost randomly distributed.

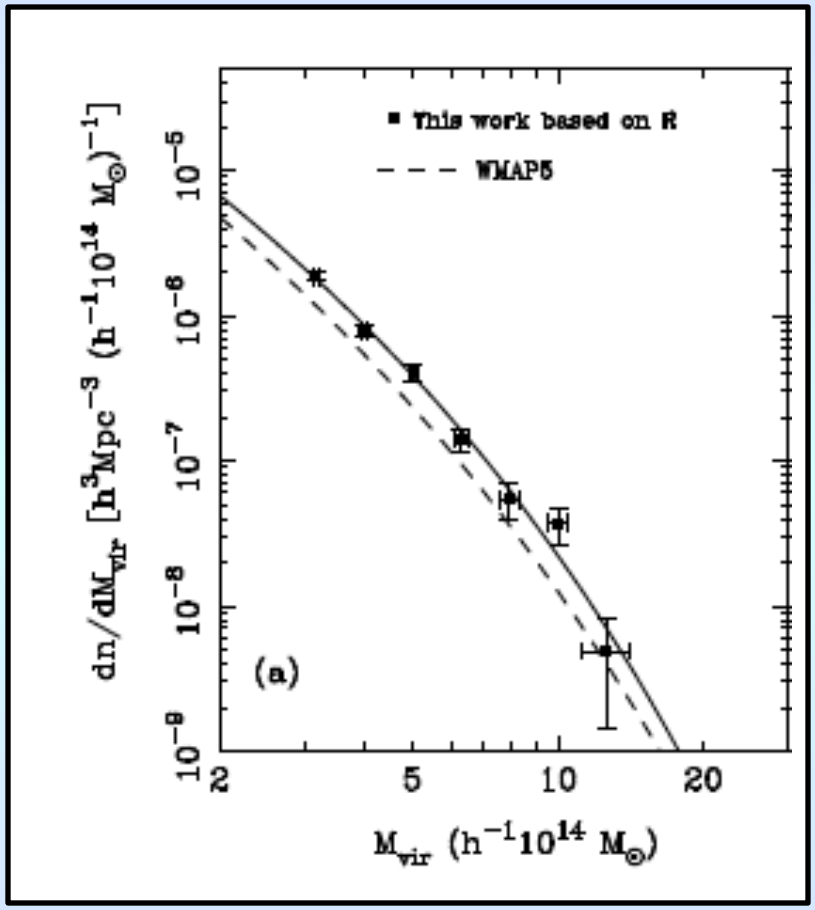

Groups and Clusters

As with most objects in the universe, there are more small galaxy groups than rich clusters. The largest bound structures in the universe are the rich galaxy clusters. These systems have masses of $\sim 10^{15}\ M_{\odot}$.

Simulations demonstrate that the greater the mass of a class of objects, the more highly clustered those objects are. The richest galaxy clusters are highly clustered; low-mass galaxies are almost randomly distributed.

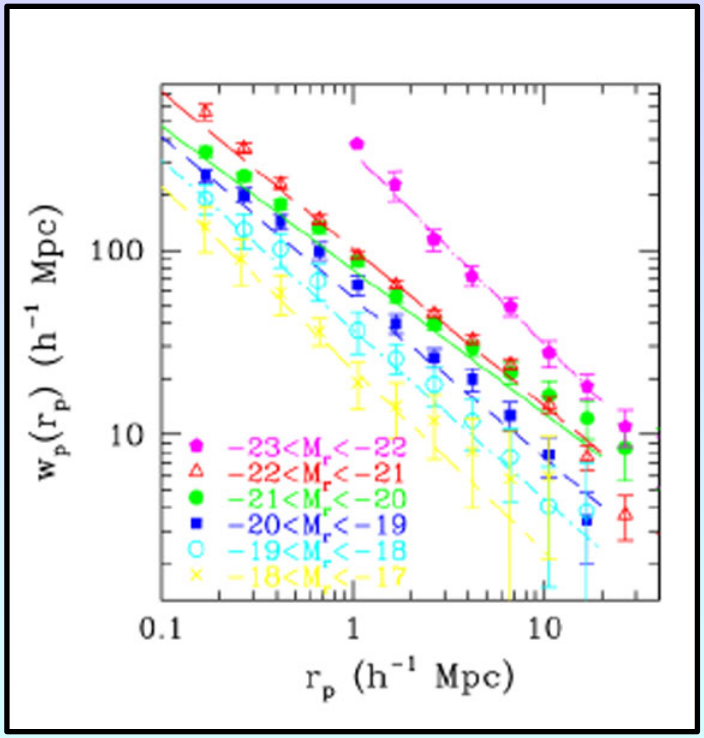

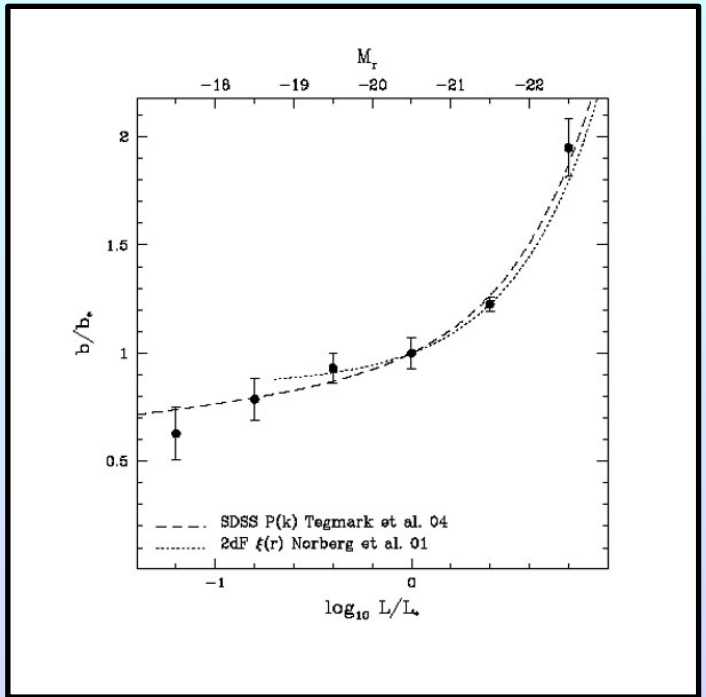

Galaxy Cluster Richness

A scale for cluster "richness" was devised by Abell (1958), who cataloged ~ 2712 rich clusters on the original Palomar Sky Survey photographic plates. (In 1989, the catalog was extended to 4073 clusters using plates from the southern hemisphere ESO Schmidt.) Abell eyeballed the plates, identified the richest clusters, and for each cluster,

- Identified the 3rd brightest galaxy (m_3)
- Estimated and subtracted off the background density of galaxies
- Estimated 2 magnitudes fainter than m_3, and counted the number of galaxies brighter than this. Based on this number, the cluster was given a Richness class:

Richness	# Galaxies	Richness	# Galaxies
0	30 - 49	3	130 - 199
1	50 - 79	4	200 - 299
2	80 - 129	5	> 300

Galaxy Cluster Condensation

Complementing the Abell system is a morphological classification defined by Bautz & Morgan in 1970. This system describes how condensed and/or (possibly) relaxed a cluster is.

Bautz-Morgan Class	Definition
I	Clusters with large, centrally located cD galaxies
II	Clusters whose brightest galaxy is intermediate between a cD galaxy and a normal elliptical galaxy
III	Clusters with no dominant galaxy

Oemler (1974) created a similar system: cD clusters have one or two cDs and a ratio of galaxy types of E/S0/S of ~3:4:2. Spiral rich clusters have field-like ratios of E/S0/S ~1:2:3, while spiral poor systems have E/S0/S ~1:4:2.

Nearby Rich Clusters

Virgo: Our closest (~ 16 Mpc) "rich" system. M87 is sometimes called the central "cD" galaxy, but in reality, the cluster has no real dominant galaxy (Bautz-Morgan III). It is too close to be included in Abell's catalog; if it were included, in would have Richness Class 0.

Centaurus: Abell 3526 is part of a network of clusters (the Centaurus supercluster) that is heavily obscured by dust in the Milky Way's plane. The system has Richness 0 (borderline Richness 1) and a Bautz-Morgan type I-II. This area is sometimes called the "Great Attractor", since its importance was first recognized via the motions of galaxies. Its distance is ~ 50 Mpc.

Coma: Abell 1656 is a Richness Class 2, Bautz-Morgan II system. At ~ 90 Mpc, it is one of the closest, rich condensed systems.

Perseus: Abell 424 is a Richness Class 2, Bautz-Morgan II-III cluster. It is slightly closer than Coma, but less condensed.

Virgo

- Irregular cluster
- Distance = 16 Mpc, closest to us
- Diameter = 10° on the sky, 3 Mpc
- ~2000 galaxies, mostly dwarfs (dEs)
- Bright galaxies – 20% ellipticals, rest are spirals (Virgo is "spiral-rich")
- Ellipticals near center, spirals in outskirts
- M87 (cD galaxy) in the center
- Virgo is very clumpy with lots of substructure; some parts of it may still be falling in, not virialized
- Hot, intracluster gas (x-ray) centered about M87
- Perhaps ~20% of Virgo's stars are outside of any galaxy

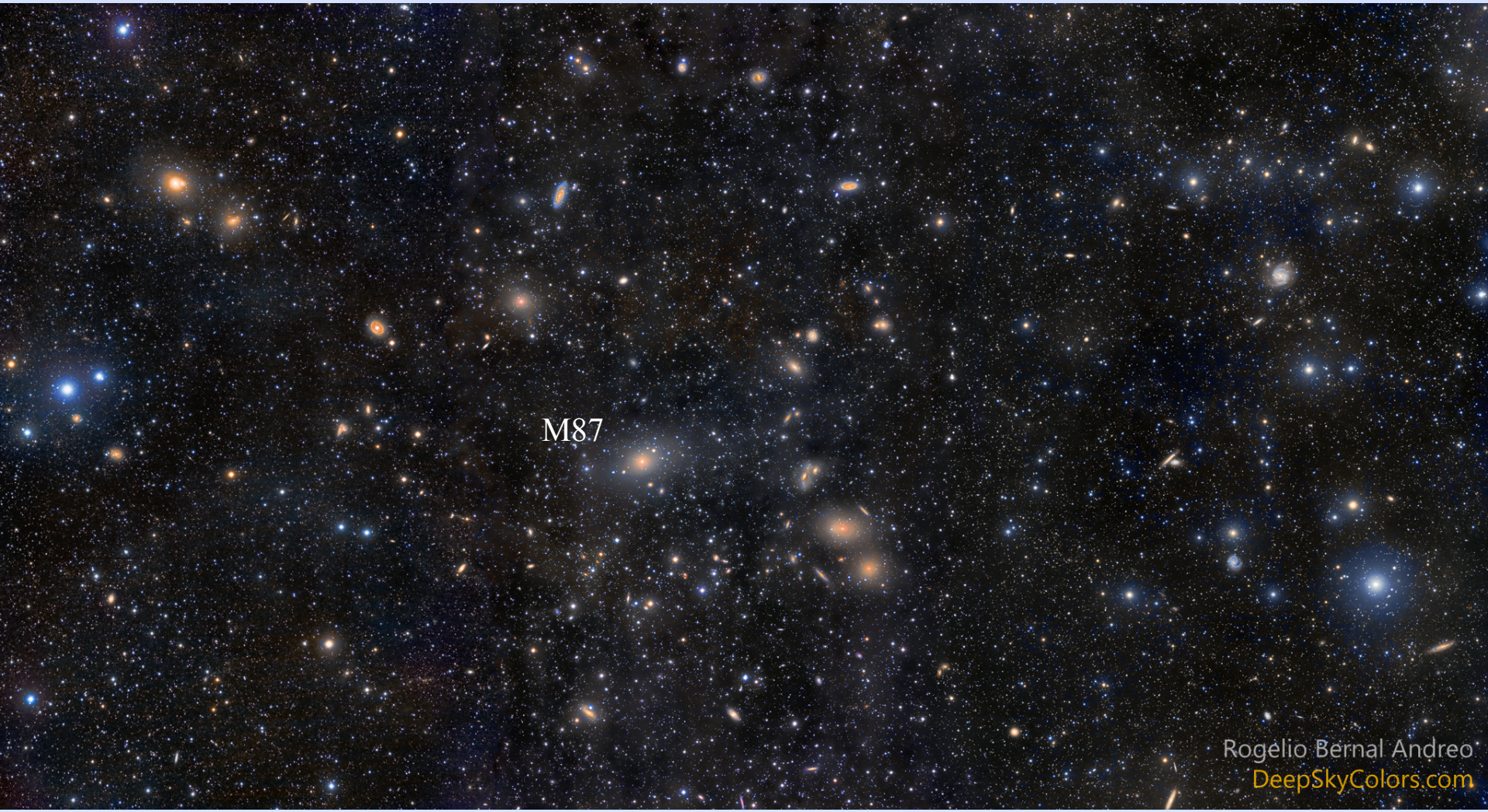
M87
Rogelio Bernal Andreo
DeepSkyColors.com

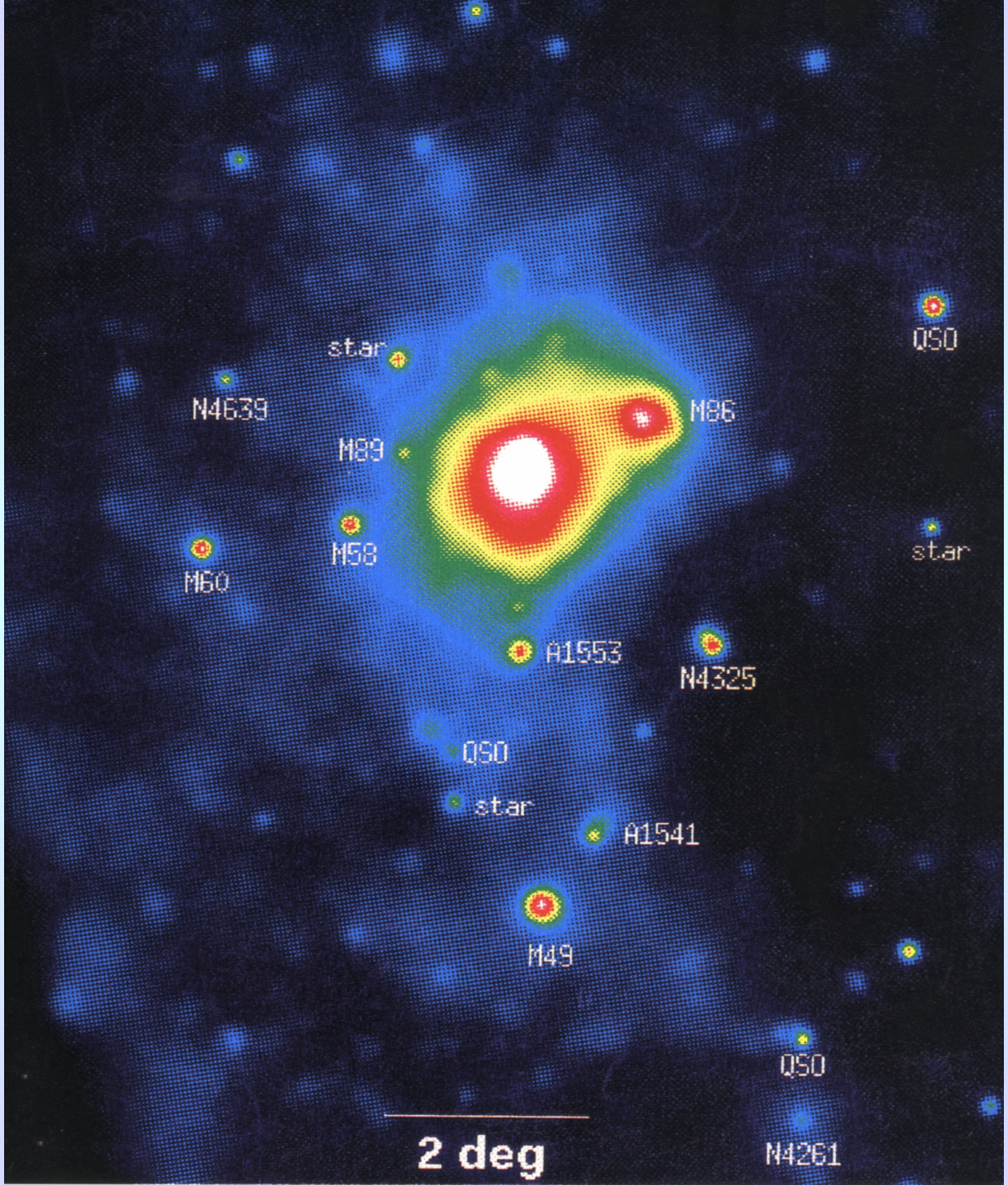
QSO
star
N4639
M86
M89
M58
M60
star
A1553
N4325
QSO
star
A1541
M49
QSO
2 deg
N4261

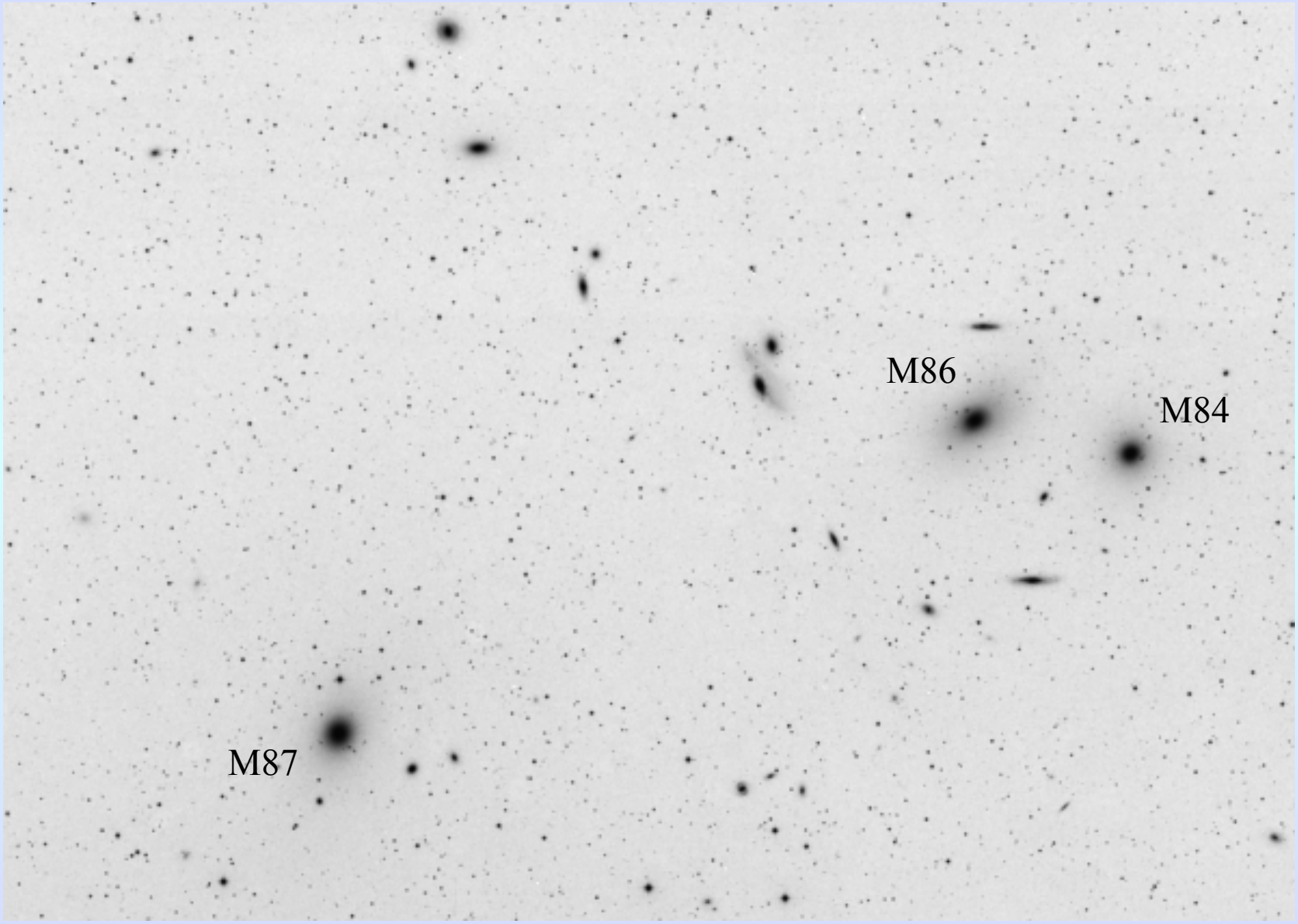
M86
M84
M87

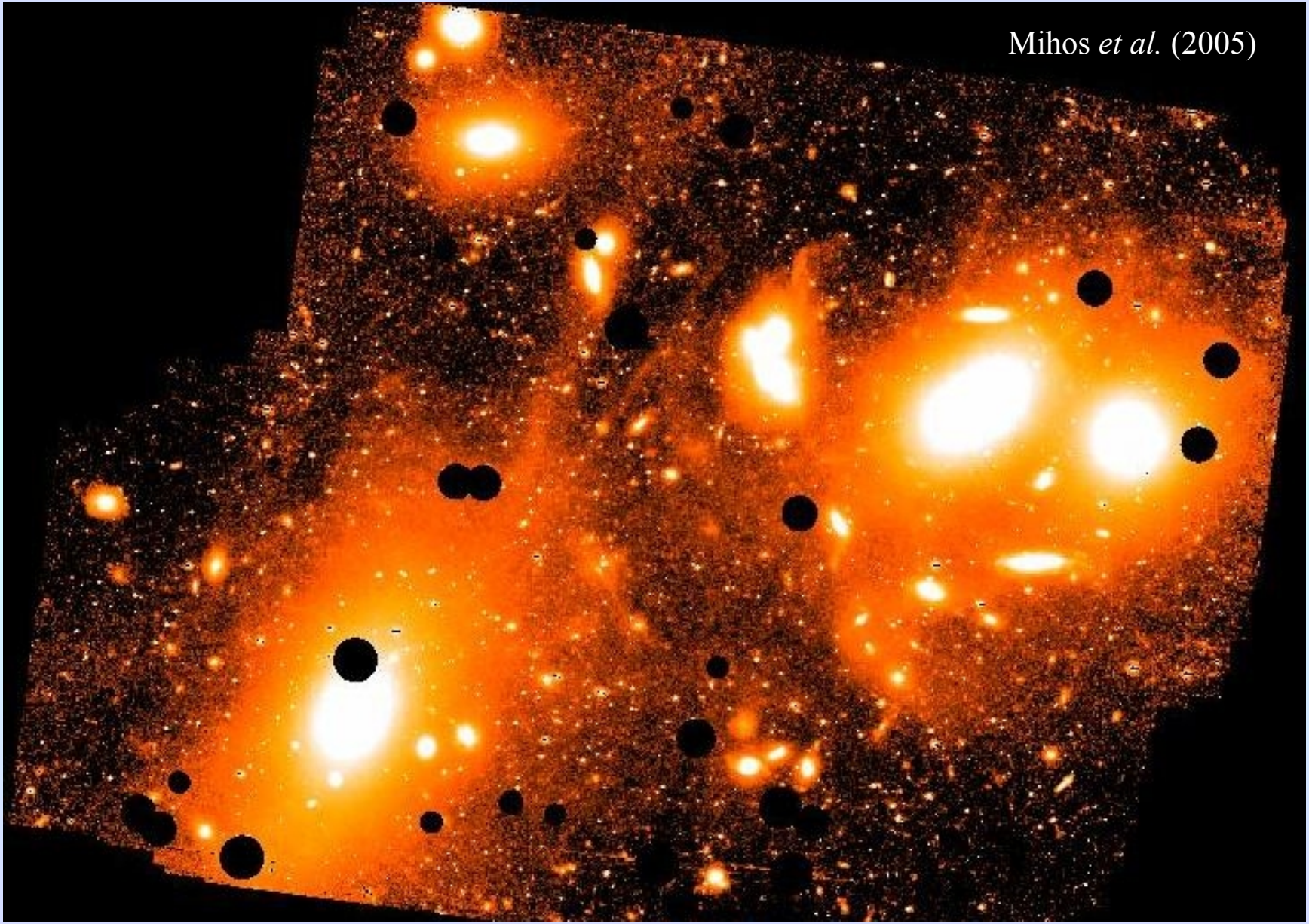
Mihos *et al.* (2005)

Centaurus

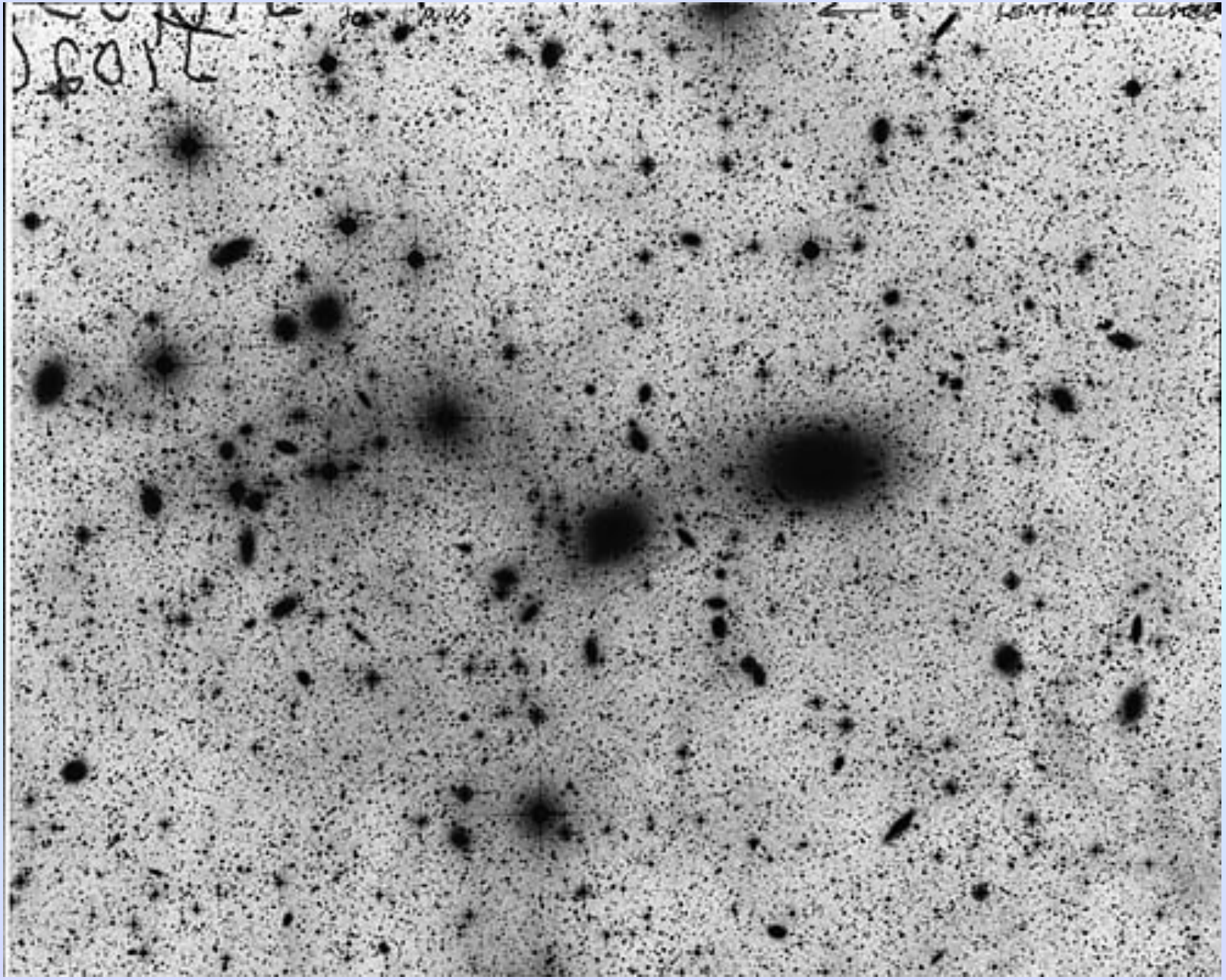

Coma

- Nearest, rich cluster of galaxies
- Distance = 90 Mpc
- Diameter = 4-5° on the sky, or 6-8 Mpc
- Population of 10,000 galaxies (but mostly dE's)
- Of the bright galaxies, <10% spirals; the rest are ellipticals or lenticulars (E/S0s)
- Roughly spherical in shape, probably virialized; 2 cD galaxies dominate in the cluster's center

Coma

Coma

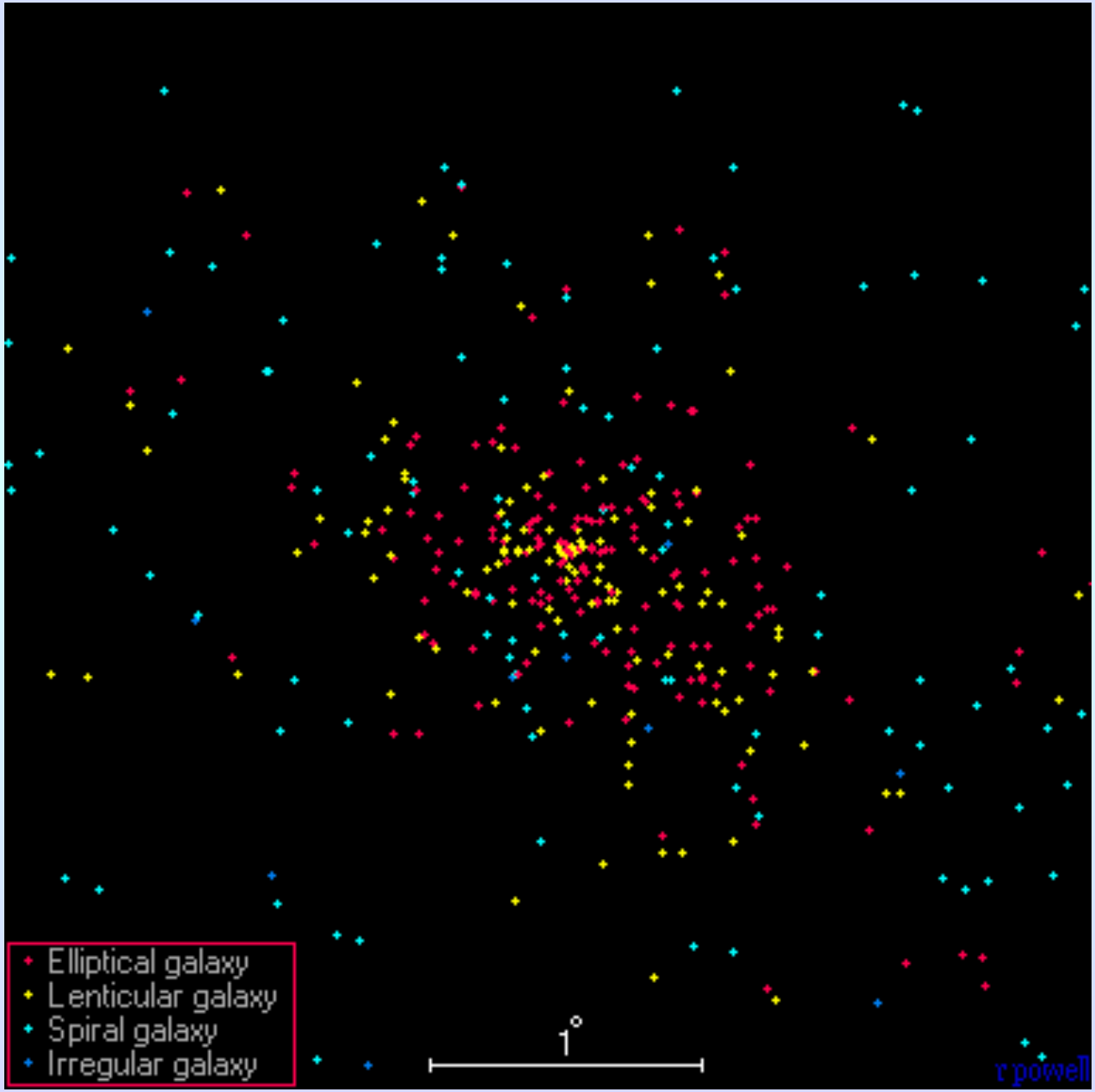
Elliptical galaxy
Lenticular galaxy
Spiral galaxy
Irregular galaxy
1°
r powell

Coma

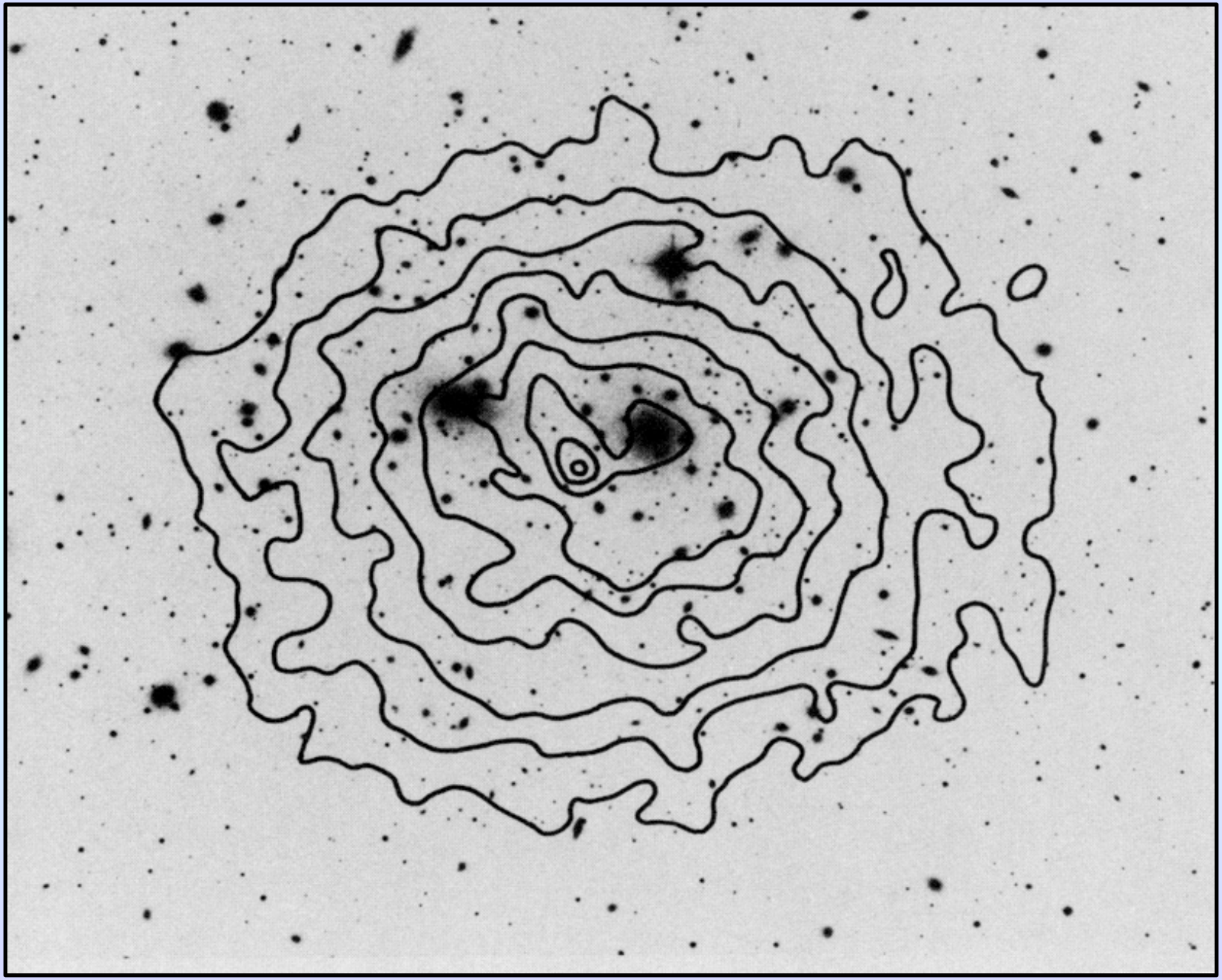

Perseus

Morphology-Density Relation

In his analysis of 6000 galaxies in 55 rich clusters and 15 "field" regions, Dressler (1980) noticed that both relaxed and irregular clusters followed the same morphology-density relation. (His work was later extended to poorer groups.)

- Dressler found that the key parameter is local density (not radius with in the cluster), where density is defined using the area enclosing the nearest 10 galaxies with $M_V < -21.4$
- The implication is that either environment affects galaxy formation (E/S0's only form in dense regions), or that spirals get converted into ellipticals in dense environments.

Possible relevant physical processes include merging, ram pressure stripping, and galaxy harrassment. Note that at $z \sim 0.4$, blue galaxies are found in some clusters. This is called the Butcher-Oemler effect.

Morphology-Density Relation

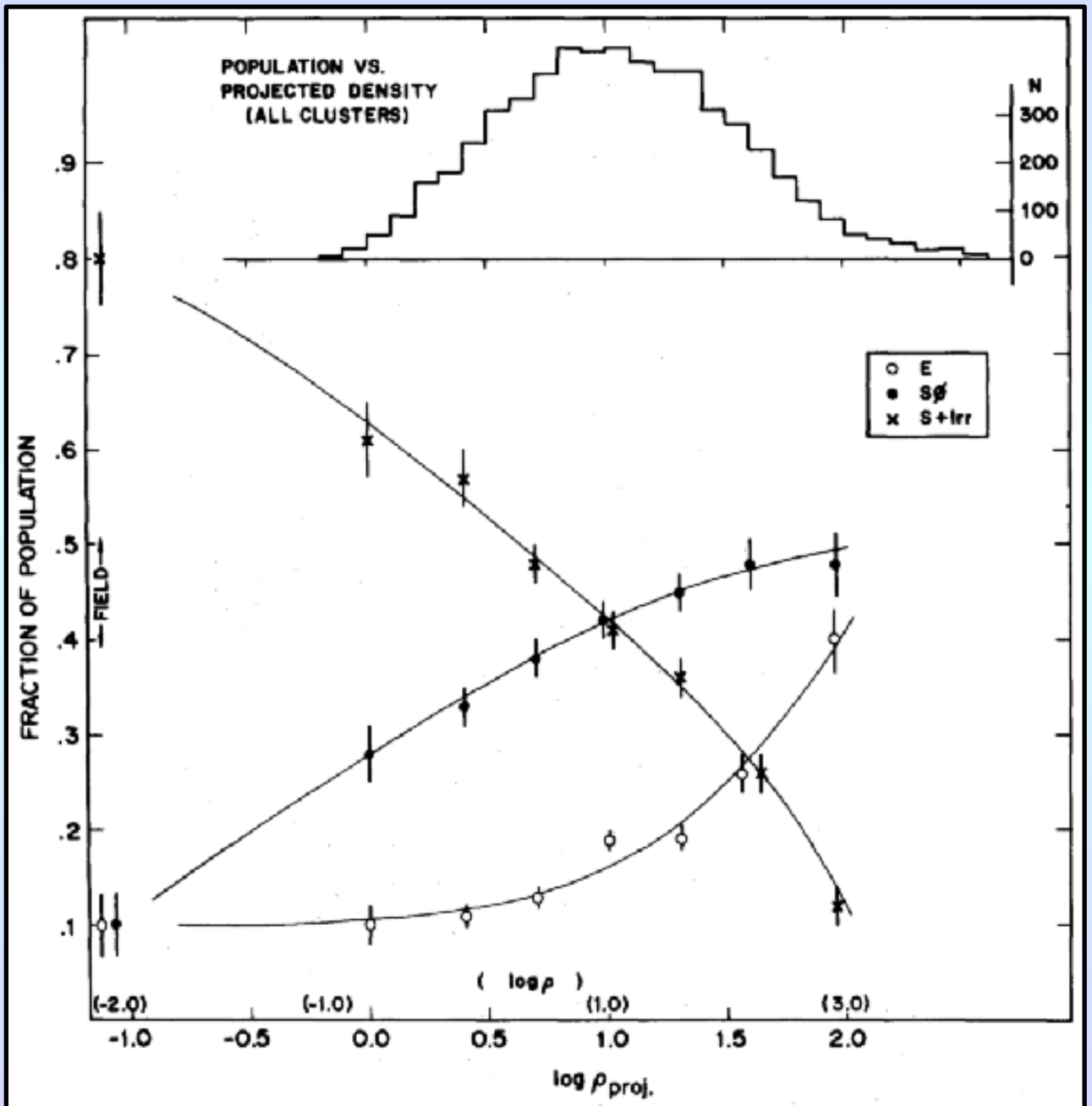

HI Gas and Tidal Stripping

Evidence for stripping of HI gas has been found in clusters. The most HI-deficient spirals are found in cluster cores, and the effect correlates with cluster X-ray luminosity. The greatest amount of stripping occurs in the outskirts of spirals. The most-likely cause is ram-pressure stripping.

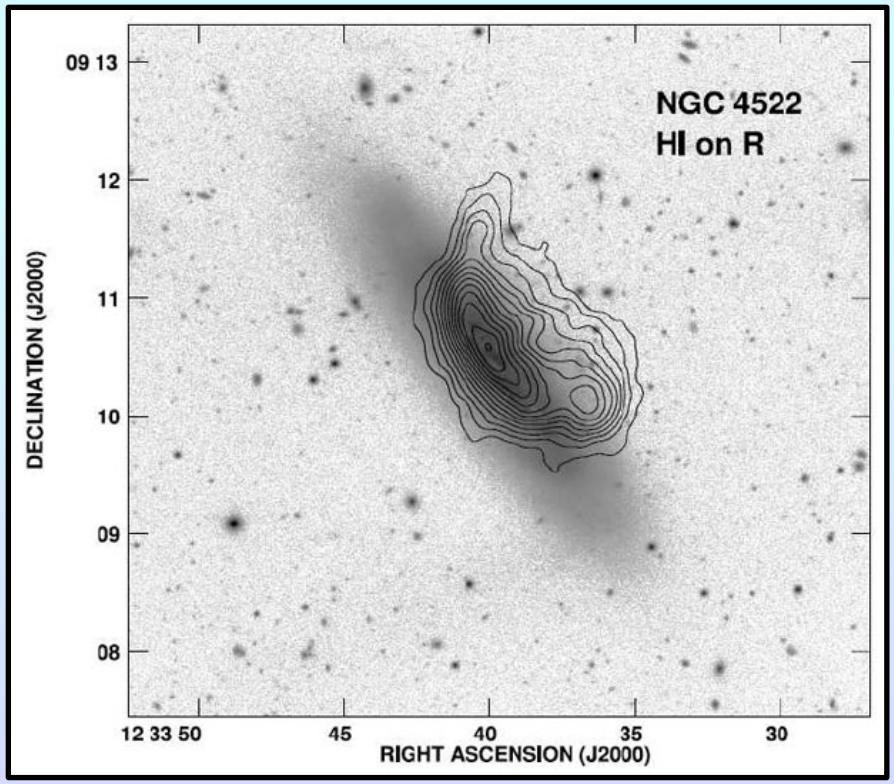

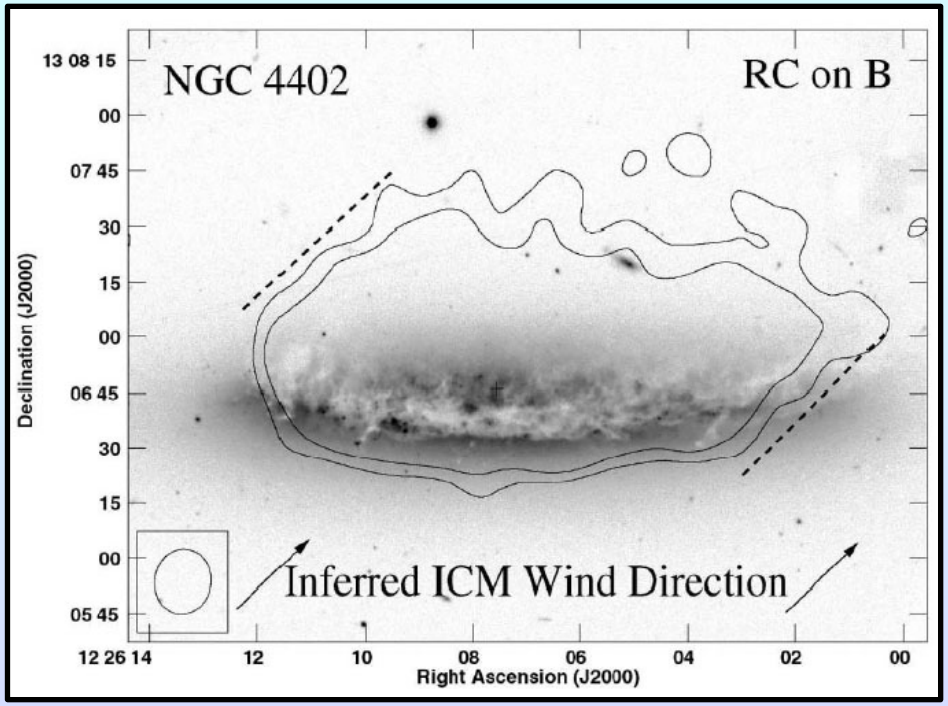

HI Gas and Tidal Stripping

Evidence for stripping of HI gas has been found in clusters. The most HI-deficient spirals are found in cluster cores, and the effect correlates with cluster X-ray luminosity. The greatest amount of stripping occurs in the outskirts of spirals. The most-likely cause is ram-pressure stripping.

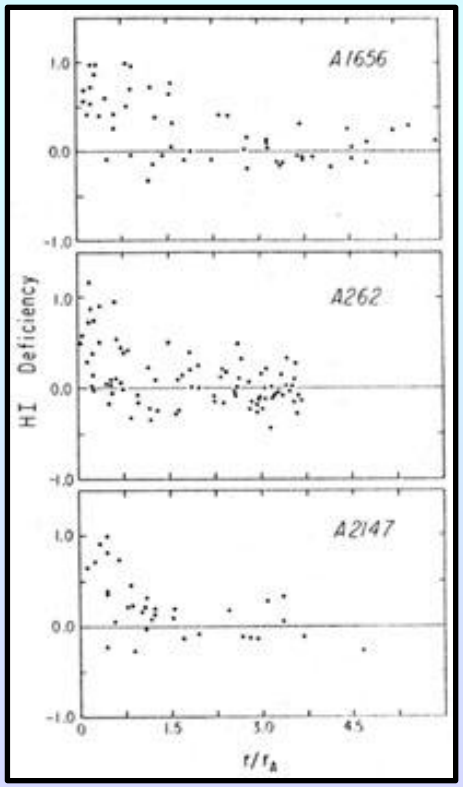

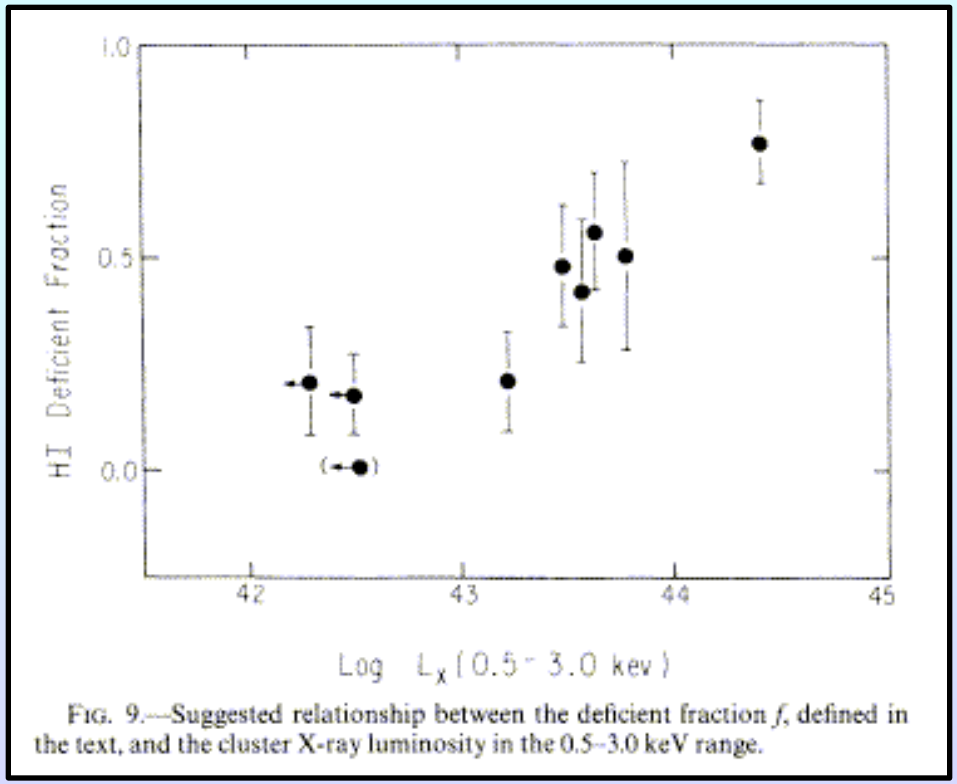

FIG. 9.—Suggested relationship between the deficient fraction *f*, defined in the text, and the cluster X-ray luminosity in the 0.5–3.0 keV range.

Galaxy Clusters and Bulk Flows

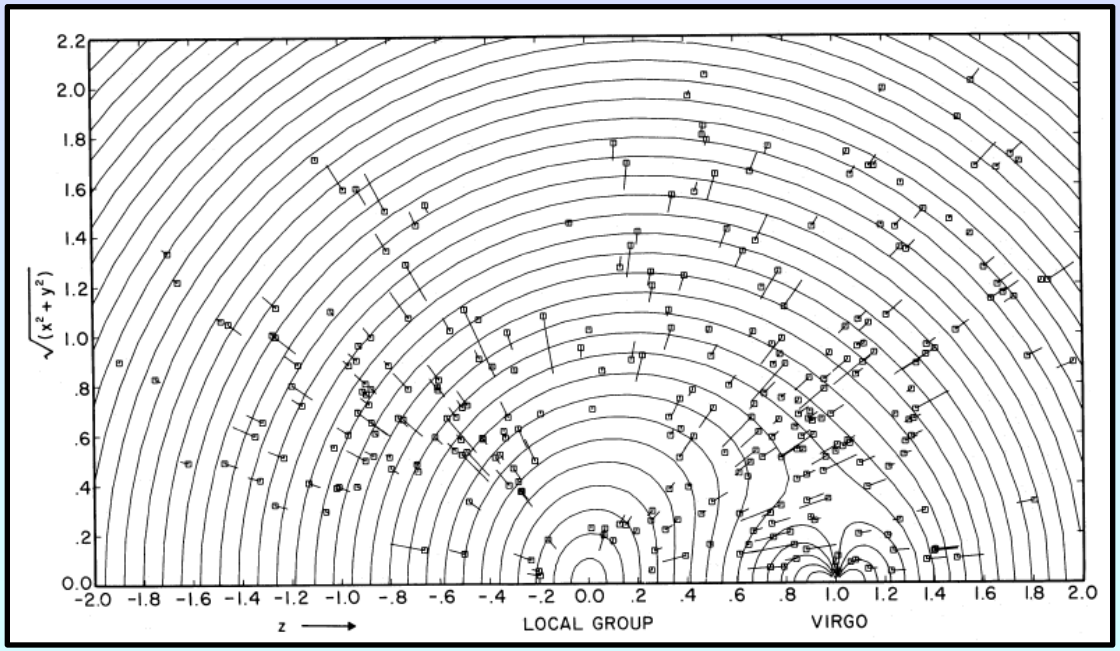

The universe is expanding with the Hubble Flow, but the masses of galaxy clusters can distort this flow (and reverse it). Galaxy clusters are the largest collapsed systems in the universe.

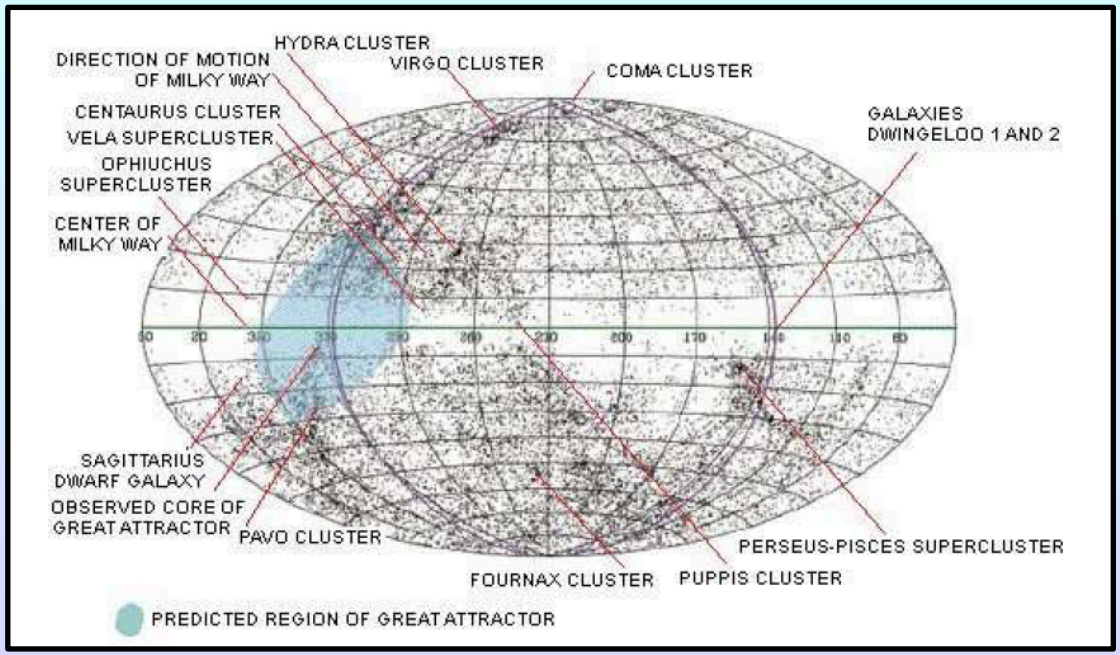

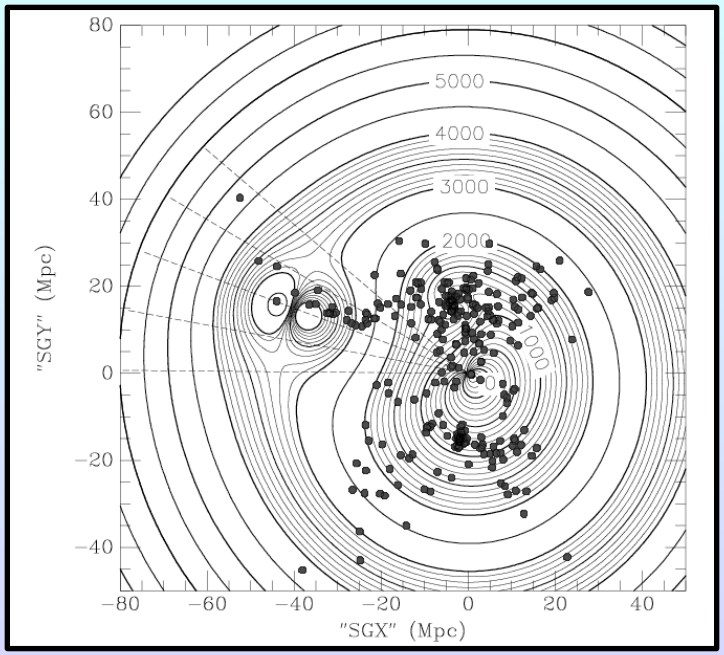

Mass Measurements of Clusters

There are 3 principle ways to measure the masses of galaxy clusters:

- From the motions of the cluster galaxies
- From the temperature of the intracluster medium
- From the distortion of background light (i.e., using a gravitational lens)

Virial Theorem

Consider a system of N particles. The moment of inertia of the system is given by

$$I = \sum_i m_i \vec{r}_i \bullet \vec{r}_i$$

If we take the 2nd derivative of this, then

$$\frac{dI}{dt} = \sum_i m_i \left(\vec{r}_i \bullet \dot{\vec{r}}_i + \dot{\vec{r}}_i \bullet \vec{r}_i \right) = \sum_i 2 m_i \vec{r}_i \bullet \dot{\vec{r}}_i$$

$$\frac{d^2 I}{dt^2} = \sum_i 2 m_i \left(\dot{\vec{r}}_i \bullet \ddot{\vec{r}}_i + \dot{\vec{r}}_i \bullet \dot{\vec{r}}_i \right)$$

or, since $\dot{\vec{r}} \bullet \dot{\vec{r}} = v^2$ and $\ddot{\vec{r}} = -\frac{GM}{r^3} \vec{r}$

$$\frac{d^2 I}{dt^2} = \sum_i 2 m_i \left(-\frac{GM}{r_i^3} \vec{r}_i \bullet \vec{r}_i + v_i^2 \right) = \sum_i 2 m_i \left(-\frac{GM}{\vec{r}_i} + v_i^2 \right)$$

Virial Theorum

For a system in steady-state equilibrium, the moment of initial shouldn't change with time, so

$$\frac{d^2 I}{dt^2} = \sum_i 2m_i \left(-\frac{GM}{r_i^3} \vec{r}_i \bullet \vec{r}_i + v_i^2 \right) = \sum_i 2m_i \left(-\frac{GM}{r_i} + v_i^2 \right) = 0$$

or

$$\sum_i -\frac{GM}{r_i} + \sum_i v_i^2 = 0$$

In other words, the potential energy plus twice the kinematic energy is zero, i.e., $\mathbf{\Omega} + 2\mathbf{T} = 0$.

Virial Theorum

The virial theorem requires knowing the object velocities and separations. However, what one measures is the objects' *radial* velocities and *projected* separations.

If you assume orbital isotropy, then the radial velocity is just one (equal) component of the total velocity, so

$$\left\langle v_{\rm rad}^2 \right\rangle = \frac{1}{3}\left\langle v^2 \right\rangle$$

Now let's consider of system of N identical mass particles. The potential term in the virial theorem is

$$\Omega = -\sum_{\text{all pairs}} \frac{Gm_i m_j}{r_{ij}} = -G\sum_{i}^{N-1} m_i^2 \sum_{j>i}^{N} \frac{1}{r_{ij}} = -Gm^2 \frac{N(N-1)}{2}\left\langle \frac{1}{r_{ij}} \right\rangle$$

To estimate $\langle 1/r \rangle$ from the mean projected separation $\langle 1/r_p \rangle$, consider that

$$r_p = r \cos i \quad \Rightarrow \quad r = r_p / \cos i \quad \Rightarrow \quad \langle 1/r \rangle = \langle 1/r_p \rangle \langle \cos i \rangle$$

and that

$$\langle \cos i \rangle = \frac{\int_0^{\pi/2} \cos i \, di}{\int_0^{\pi/2} di} = \frac{2}{\pi}$$

So

$$\Omega = -Gm^2 \frac{N(N-1)}{2} \cdot \frac{2}{\pi} \cdot \left\langle \frac{1}{r_p} \right\rangle \approx \frac{GM^2}{\pi} \left\langle \frac{1}{r_p} \right\rangle$$

The virial theorem then says

$$2T = \Omega \quad \Rightarrow \quad M \cdot 3\left\langle v_{rad}^2 \right\rangle = \frac{GM^2}{\pi} \left\langle \frac{1}{r_p} \right\rangle \quad \Rightarrow \quad M = \frac{3\pi \left\langle v_{rad}^2 \right\rangle}{G \left\langle 1/r_p \right\rangle}$$

Virial Theorem in Practice

In practice, one can never measure the radial velocity of every object in a system. Instead, one measures a set of test particles. In this case, the most important contributor to the potential is not any of the particles, but the system itself.

Consider a particle at radius r_i. This particle will feel the potential of all the mass interior to r_i, so

$$\Omega = -G\sum_{i=1}^{N}\frac{M(r_i)m_i}{r_i}$$

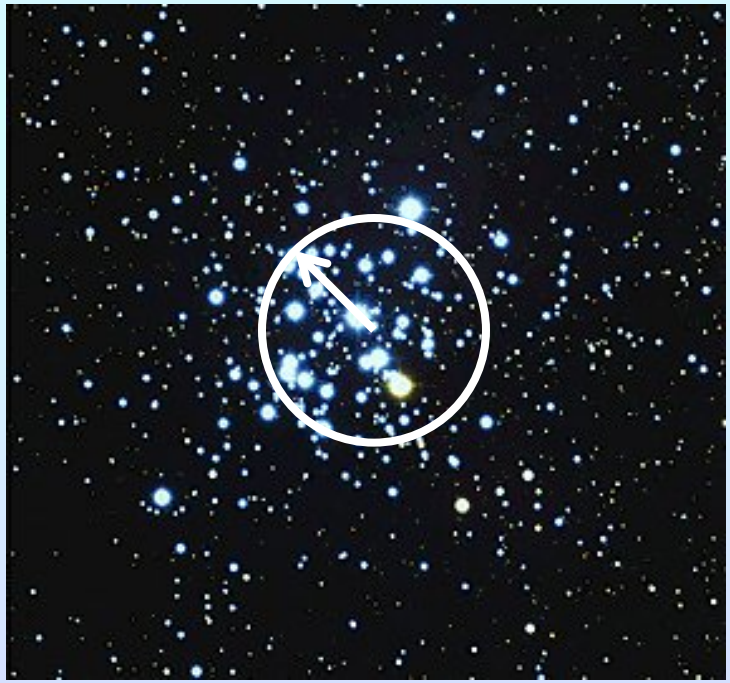

As before, $\langle 1/r \rangle = \langle 1/r_p \rangle\ (2/\pi)$, so

$$\Omega = \frac{2G}{\pi}\langle M \rangle \left\langle \frac{1}{r_p} \right\rangle$$

where $\langle M \rangle$ is the mean enclosed mass for the particles.

Virial Theorum in Practice

Again, for isotropic orbits, the kinetic energy is 3 times the radial velocity dispersion, so

$$\langle M \rangle = \frac{3\pi}{2G} \frac{\left\langle v_{rad}^2 \right\rangle}{\left\langle 1/r_p \right\rangle}$$

Note that because you are now only measuring $\langle M \rangle$, a model of the system is needed to derive total mass. (Either that, or only use particles at large radius.) Also note that if the test particles have significantly different masses, then

$$\langle M \rangle = \frac{3\pi}{2G} \left(\sum_{i=1}^{N} m_i v_{i,rad}^2 \right) \Big/ \left(\sum_{i=1}^{N} \frac{m_i}{r_{p\,i}} \right)$$

Limitations of the Virial Theorem

For most astronomical applications, the Virial Theorem is imperfect. For instance

- The results are biased: if one performs a time-average over a circular orbit, then from Page (1952)

$$v_{rad}^2 r_p = \frac{3\pi}{32} v^2 r$$

so for a system of randomly oriented circular orbits

$$M_{VT} = \frac{9\pi^2}{64} M_{true} = 1.388 M_{true}$$

Similarly, for a system of randomly oriented radial orbits,

$$M_{VT} = \frac{3\pi^2}{64} M_{true} = 0.463 M_{true}$$

Limitations of the Virial Theorem

For most astronomical applications, the Virial Theorum is imperfect. For instance

- The technique is inefficient: the error associated with M_{VT} is proportional to that of the mean projected radius, i.e.,

$$M_{VT} = \frac{3\pi}{2G}\frac{\left\langle v_{rad}^2 \right\rangle}{\left\langle 1/r_p \right\rangle} \quad \Rightarrow \quad \sigma_{VT}^2 \propto \sigma_{\langle 1/r_p \rangle}^2$$

By definition

$$\sigma_{\langle 1/r_p \rangle}^2 = \left\langle \frac{1}{r_p^2} \right\rangle - \left\langle \frac{1}{r_p} \right\rangle^2 \quad \text{and} \quad \left\langle \frac{1}{r_p^2} \right\rangle \propto \left\langle \frac{1}{r^2 \cos^2 i} \right\rangle = \left\langle \frac{1}{r^2} \right\rangle \left\langle \frac{1}{\cos^2 i} \right\rangle = \left\langle \frac{1}{r^2} \right\rangle \left\langle \sec^2 i \right\rangle$$

But

$$\left\langle \sec^2 i \right\rangle = \frac{\int_0^{\pi/2} \sec^2 i \, di}{\int_0^{\pi/2} di} = \frac{\tan i \Big]_0^{\pi/2}}{\pi/2} \Rightarrow \text{ an infinite dispersion!!!}$$

Limitations of the Virial Theorem

For most astronomical applications, the Virial Theorum is imperfect. For instance

- Even with an infinite number of particles, the mass may not converge. Suppose the true density of objects goes as r^{-s}. By definition, the harmonic mean radius, $\langle 1/r \rangle$ is

$$\left\langle \frac{1}{r} \right\rangle = \frac{\int_0^R \left(\frac{1}{r}\right) 4\pi r^2 \cdot r^{-s}\, dr}{\int_0^R 4\pi r^2 \cdot r^{-s}\, dr} \propto \frac{r^{2-s}\Big|_0^R}{r^{3-s}\Big|_0^R}$$

For $2 < s < 3$, the denominator is finite, but the mean quantity $\langle 1/r \rangle$ is infinite.

Suggested Virial Theorem Alternative

Bahcall & Tremaine (1981) and Heisler et al. (1985) suggest an alternative to the classical virial theorem. Based on hydrodynamic simulations of spherical systems, they developed a projected mass estimator

$$M_{PM} = \frac{f_{PM}}{GN} \sum_{i=1}^{N} v_r^2 \, r_p \quad \text{with} \quad f_{PM} = \frac{32}{\pi} \quad \text{for isotropic orbits}$$

$$f_{PM} = \frac{64}{\pi} \quad \text{for radial orbits}$$

The Mass of Clusters

The first virial mass estimate of a galaxy cluster was by Zwicky in 1937 (using just 8 galaxies)! His inferred mass of $M > 5 \times 10^{14}\ M_{\odot}$ for Coma implied 90% of the cluster's mass was invisible. In general, this wasn't considered to be a problem (in part, because he was Fritz Zwicky).

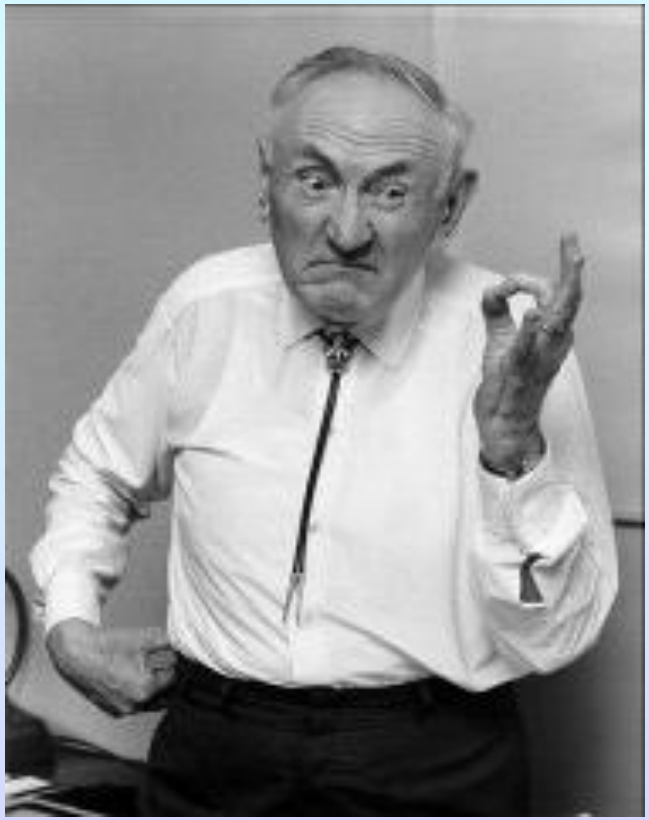

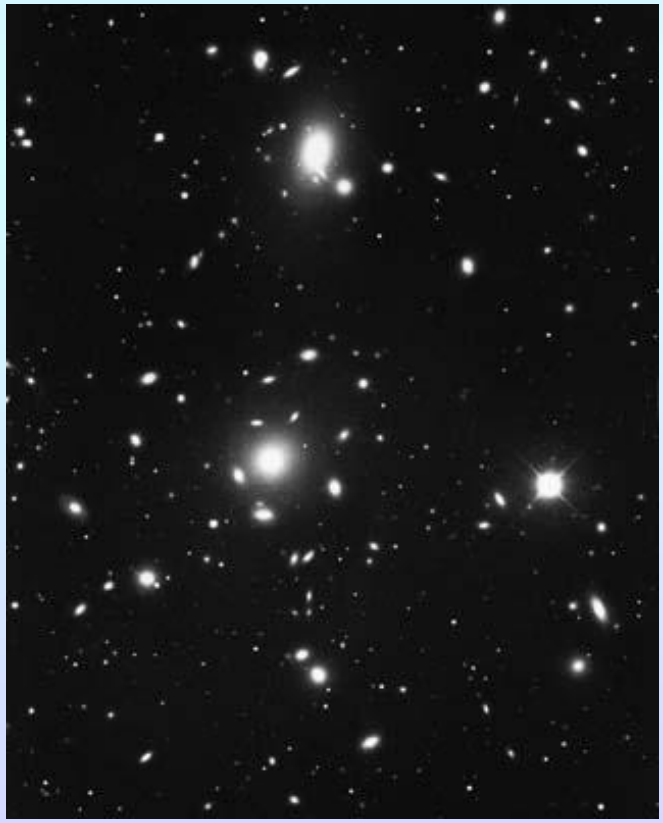

Are Clusters Virialized?

Is virial equilibrium a good assumption? For example, from the spatial and velocity distribution of galaxies, the Virgo Cluster looks virialized.

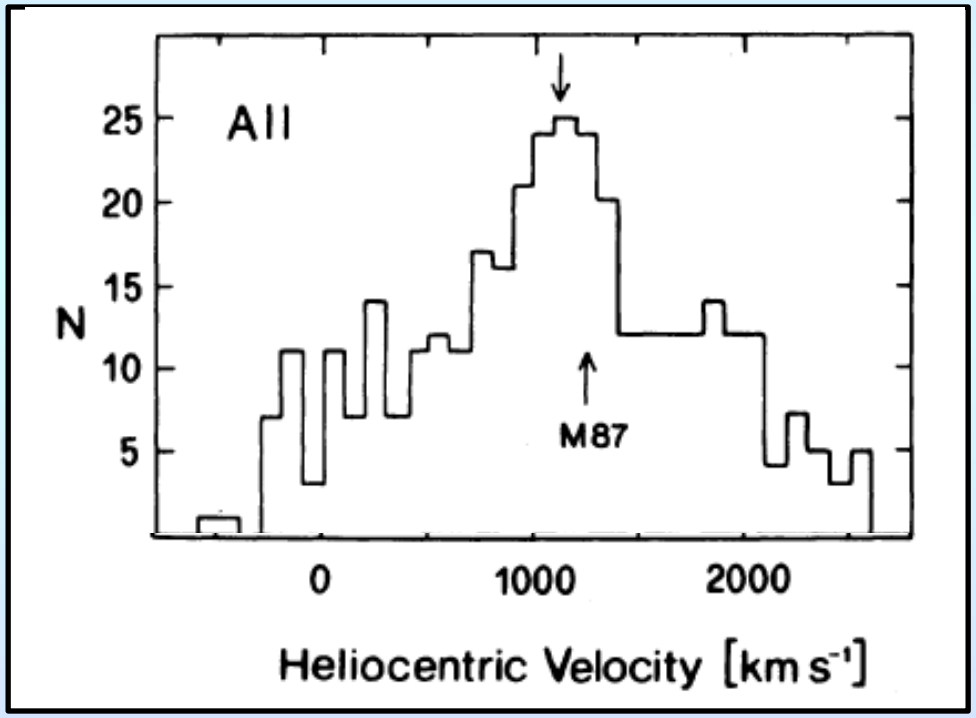

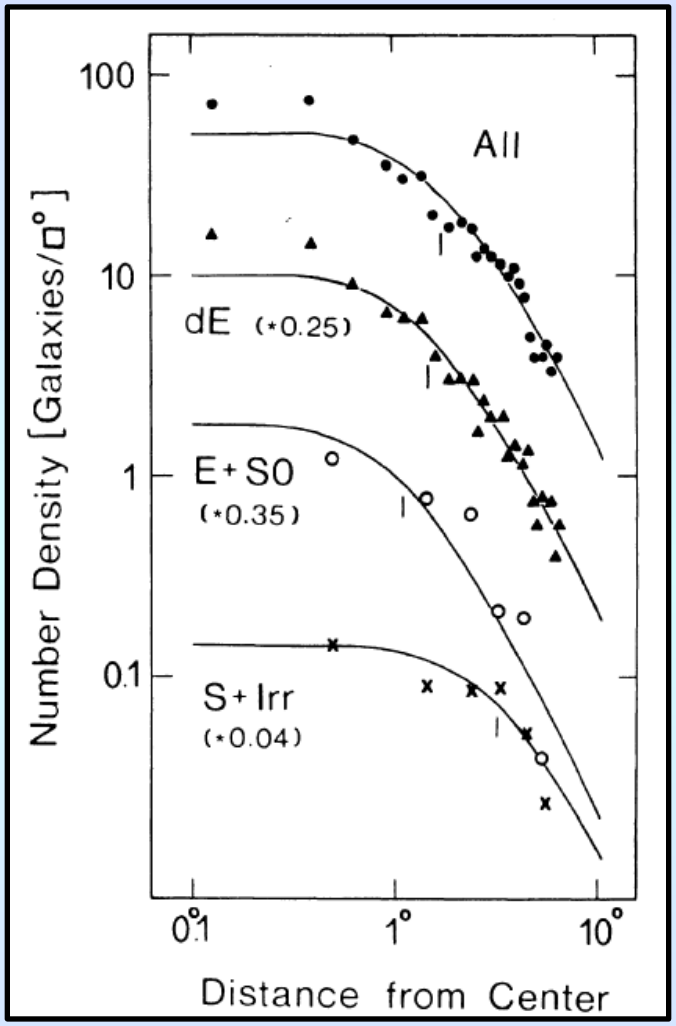

Are Clusters Virialized?

Is virial equilibrium a good assumption? For example, from the spatial and velocity distribution of galaxies, the Virgo Cluster looks virialized.

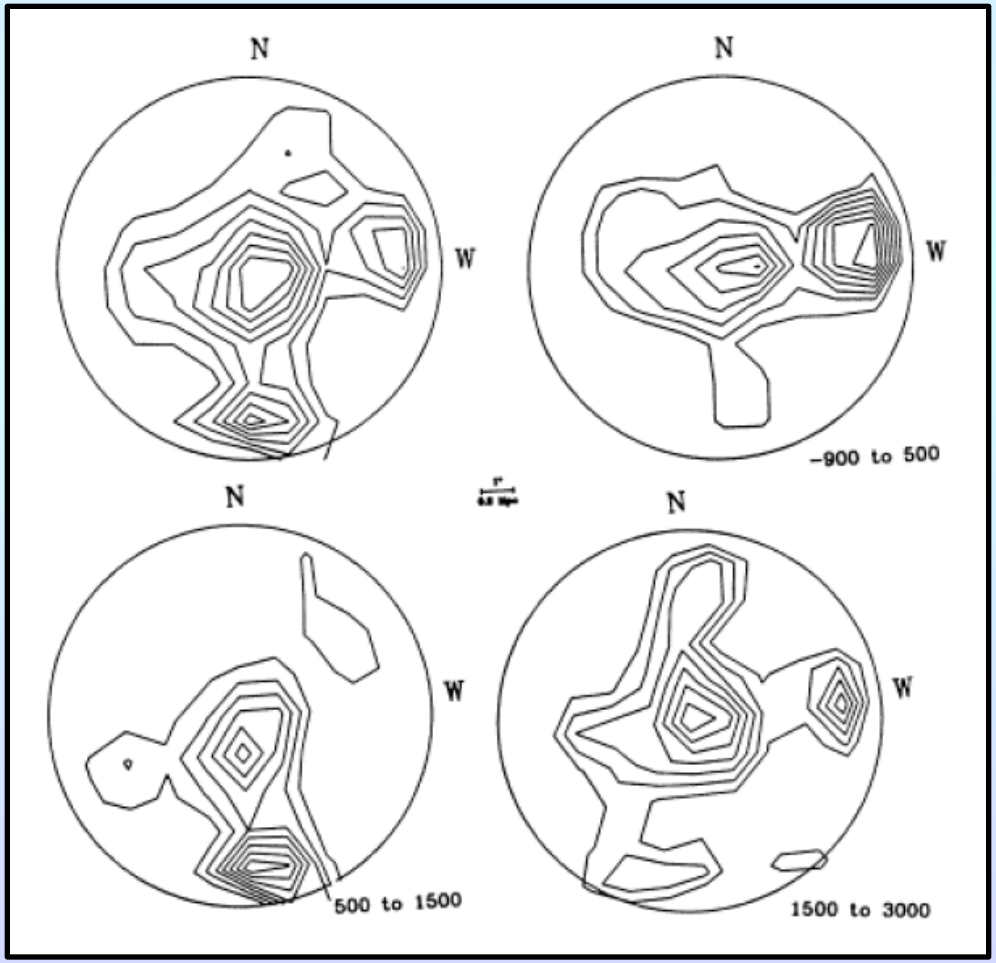

But a closer examination show that Virgo contains a number of sub-clumps. Although some areas of the cluster may be relaxed, the system, as a whole, is not yet virialized.

The Intracluster Medium

Galaxies only contain about 20% of the baryons present in rich clusters. The other ~ 80% resides in the intracluster medium. The intracluster medium can be built up in 4 ways:

1) Gas can fall into the cluster as it forms.
2) Gas can be blown out of small galaxies by winds.
3) Gas can be ejected from galaxies by AGN jets and winds.
4) Gas can be swept out by ram pressure ($\rho_x v^2 > F_{grav} \sigma_{gas}$).

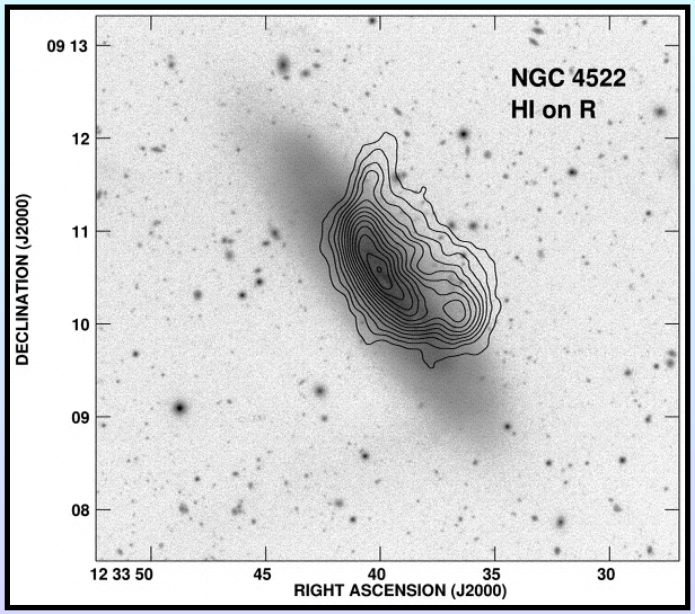

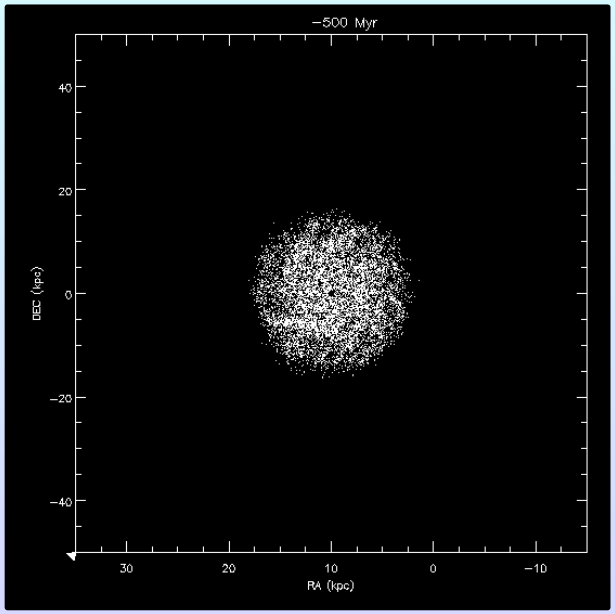

The X-ray Gas

Let's consider the temperature of the intracluster gas. A typical rich cluster will have a mass of ~ $10^{15}\ M_{\odot}$, and radius of ~ 1 Mpc. Gas falling into this cluster (or ejected from galaxies moving in the cluster potential) will therefore thermalize with an initial temperature of

$$\frac{GMm_H}{R} \sim \frac{1}{2} m_H v^2 \sim \frac{3}{2} kT \quad \Rightarrow \quad T \sim 10^8 \text{ K}$$

This gas is very hot – hotter than the center of the Sun – and will emit X-rays.

The X-ray Gas

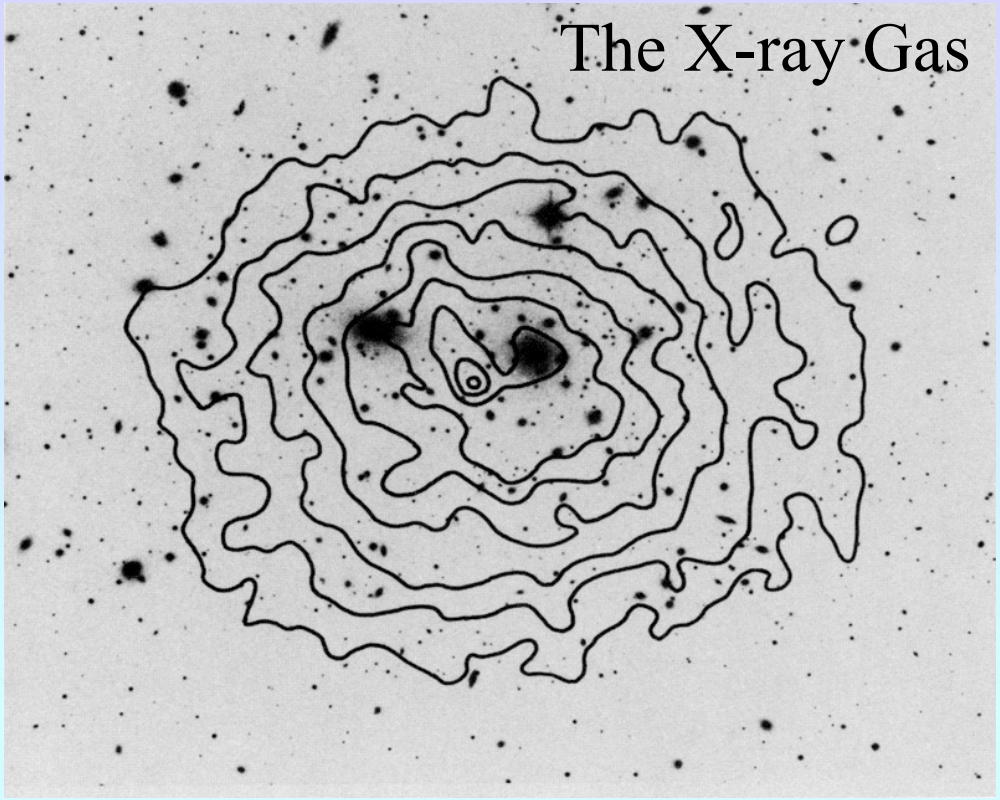

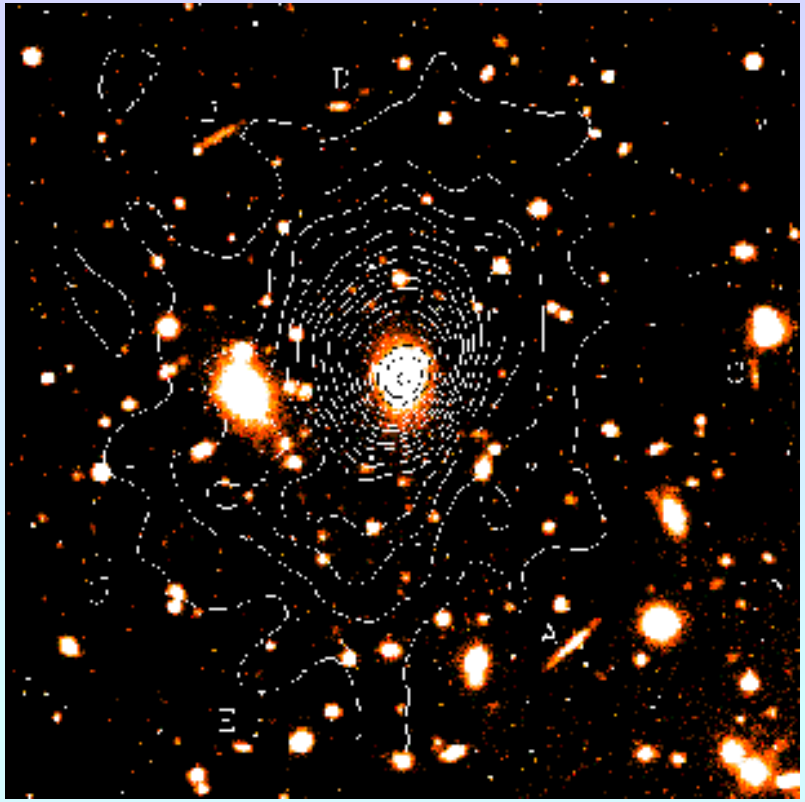

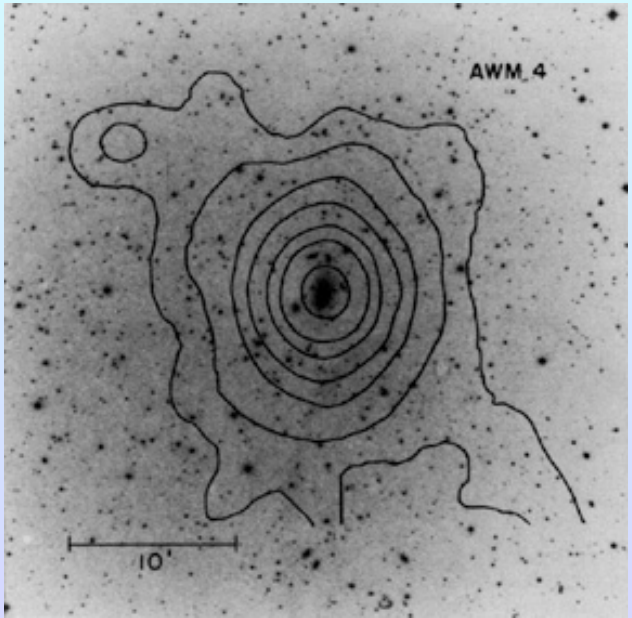

The Electron Mean Free Path

Consider an electron (or ion) moving in this plasma. The path of the particle will be deflected by other charged particles in the plasma. We can calculate the particle's mean free path in *exactly* the same way as for stellar relaxation times. If Λ is ratio of the largest to the smallest impact parameters, and n the particle density, then

$$\lambda = \frac{3^{3/2}(kT)^2}{4\pi^{1/2} n e^4 \ln\Lambda} \quad \text{with} \quad \ln\Lambda = 37.8 + \ln\left\{\left(\frac{T}{10^8}\right)\left(\frac{n_e}{10^{-3}\ \mathrm{cm}^{-3}}\right)^{-1/2}\right\}$$

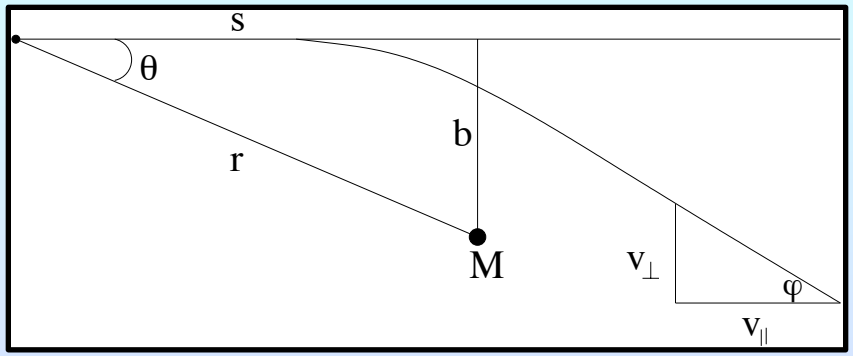

$$\lambda_e \sim \lambda_i \sim 23\left(\frac{T}{10^8}\right)^2\left(\frac{n_e}{10^{-3}\ \mathrm{cm}^{-3}}\right)^{-1}\ \mathrm{kpc}$$

A typical cluster has an ICM density of $\sim 10^{-3}$ cm^{-3}. A particle can travel the length of a galaxy and not interact with anything!

The Timescale for Equipartition

Since the mean free path is known, we can now calculate the timescale for the particle to thermalize into the system's Maxwellian velocity curve. This is simply

$$t_{eq} = \lambda / v = \lambda / \sqrt{\frac{3kT}{m}} = \frac{3m^{1/2}\left(kT\right)^{3/2}}{4\pi^{1/2} n e^4 \ln\Lambda}$$

For proton-proton interactions, this is

$$t_{eq}^{+} = 1.4 \cdot 10^7 \left(\frac{T}{10^8}\right)^{3/2} \left(\frac{n_e}{10^{-3}\ \mathrm{cm}^{-3}}\right)^{-1} \ \mathrm{yr}$$

while for electron-electron interactions, it is

$$t_{eq}^{-} = 3.3 \cdot 10^5 \left(\frac{T}{10^8}\right)^{3/2} \left(\frac{n_e}{10^{-3}\ \mathrm{cm}^{-3}}\right)^{-1} \ \mathrm{yr}$$

Note: for a typical density of 10^{-3} cm^{-3}, this timescale is short!!!

The Timescale for Cooling

At a temperature of ~ 10^8 K, atoms are almost completely ionized, so collisional cooling is not as important as for the warm ISM.

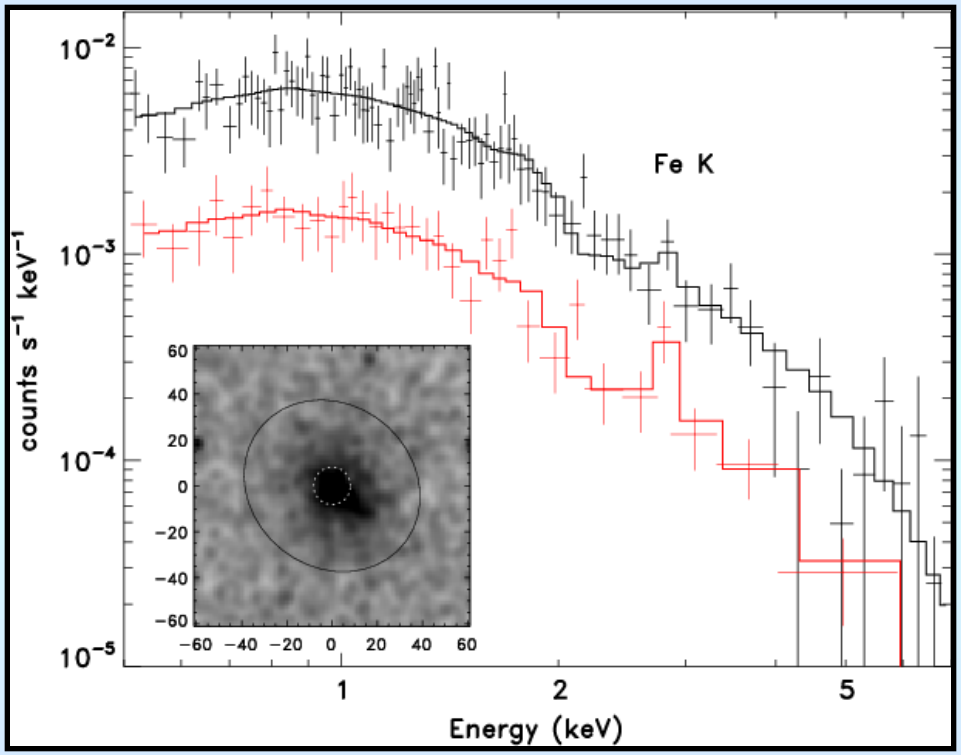

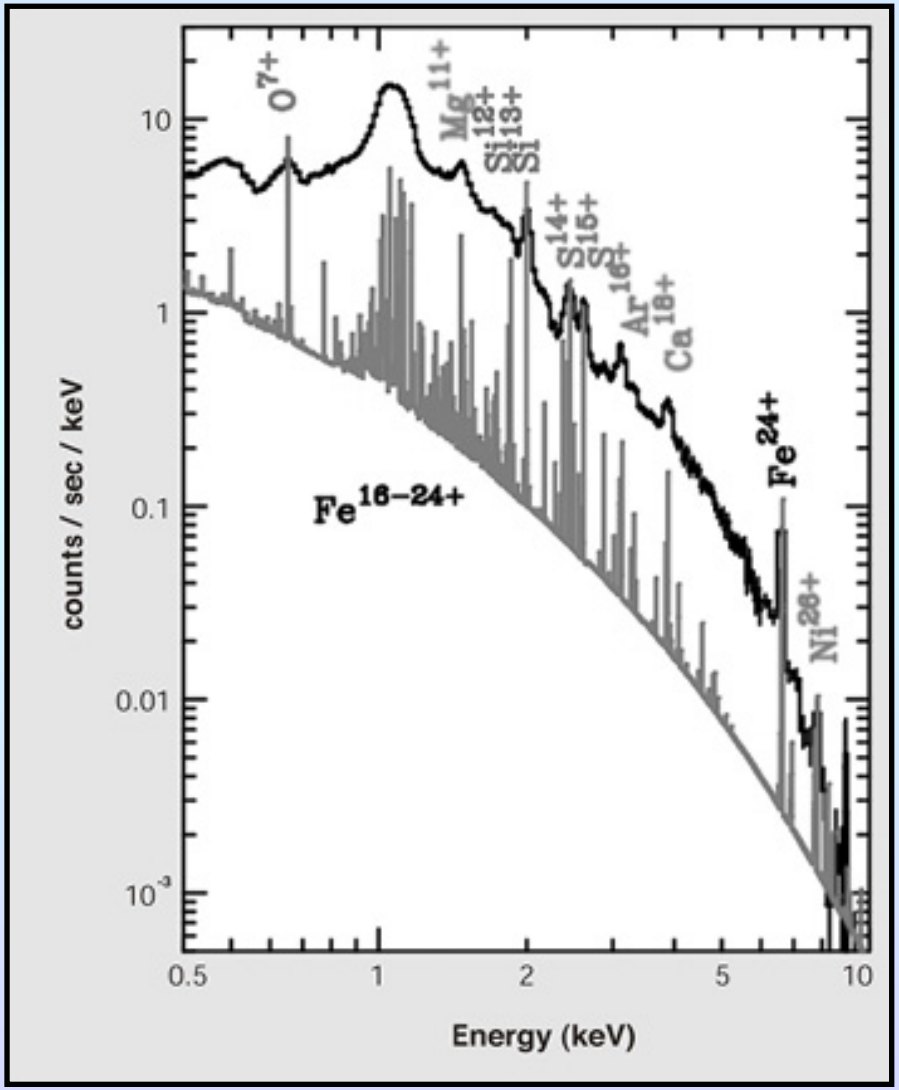

Collisional cooling is only a few times more important than free-free cooling.

The Timescale for Cooling

The cooling timescale for a gas a simply

$$t_{cool} = T / \frac{dT}{dt} = \left(\frac{d \ln T}{dt} \right)^{-1}$$

In the case of free-free emission, the emissivity is

$$\varepsilon_{ff} = \frac{dE}{dt} = \frac{3}{2} nk \frac{dT}{dt} = \frac{32\pi e^6}{3 m_e c^3} \left(\frac{2\pi}{3 m_e kT} \right)^{1/2} Z^2 n_i n_e \int_0^\infty g_{ff} e^{-h\nu / kT} d\nu$$

$$= \frac{32\pi e^6}{3 h m_e c^3} \left(\frac{2\pi k}{3 m_e} \right)^{1/2} \bar{g}\, n_e T^{1/2} \sum_i Z_i^2 n_i$$

$$\sim 3 \times 10^{-27} n_p^2 T^{1/2} \text{ ergs cm}^{-3} \text{ s}^{-1}$$

(for solar-type metallicity). As with most cooling mechanisms, the dependence is on density-squared, and the square-root of temperature.

The Timescale for Cooling

The cooling time of a gas is then

$$t_{cool} = T / \frac{dT}{dt} = \left(\frac{d \ln T}{dt} \right)^{-1} = T / \left(\frac{2\varepsilon_{ff}}{3 k n_p} \right)$$

$$= \frac{k T^{1/2}}{2 \times 10^{-27} n_p} = 22 \times 10^9 \left(\frac{T}{10^8} \right)^{1/2} \left(\frac{n_e}{10^{-3} \mathrm{cm}^{-3}} \right)^{-1} \mathrm{yr}$$

For a typical cluster, the free-free cooling time is more than the age of the universe! Collisional cooling may be several times more important, but (except in cluster cores where the ICM density may be high), the cooling time will still be very long.

The Timescale for Pressure Equilibrium

Finally, let's ask how long it takes a pressure wave to cross a cluster and distribute any inhomogeneity over the system. This is simply the cluster size divided by the sound speed

$$t_p = D/c_s = D/\sqrt{\frac{\gamma P}{\rho}} = D/\sqrt{\frac{\gamma kT}{\mu m_H}}$$

where γ=5/3 is the ratio of the specific heats and μ~1 is the mean molecular weight. So

$$t_p = 6.5\times10^8 \left(\frac{T}{10^8}\right)^{-1/2}\left(\frac{D}{\mathrm{Mpc}}\right)\mathrm{yr}$$

Again, this timescale is very short, compared to a Hubble time. The X-ray gas should therefore be hot and in both thermal and pressure equilibrium.

X-ray Gas and Hydrostatic Equilibrium

Given that an X-ray gas is in thermal and pressure equilibrium, it is fairly straightforward to use the distribution of gas to derive the mass distribution of the cluster. Begin with the equation of hydrostatic equilibrium

$$\frac{dP}{dr} = -g\rho = -\frac{GM(r)}{r^2}\rho$$

The pressure derivative can be written in terms of the ideal gas equation, so

$$P = \frac{k}{\mu m_H}\rho T \quad \Rightarrow \quad \frac{dP}{dr} = \frac{k}{\mu m_H}\left\{T\frac{d\rho}{dr} + \rho\frac{dT}{dr}\right\}$$

Now if we equate the two equations, we get a simple expression for the total mass of the cluster:

$$-\frac{GM(r)}{r^2}\rho = \frac{k}{\mu m_H}\left\{T\frac{d\rho}{dr} + \rho\frac{dT}{dr}\right\}$$

$$-\frac{GM(r)}{r} = \frac{kT}{\mu m_H}\left\{\frac{r}{\rho}\frac{d\rho}{dr} + \frac{r}{T}\frac{dT}{dr}\right\}$$

$$M(r) = -\frac{kT}{\mu m_H G}\left\{\frac{d\ln\rho}{d\ln r} + \frac{d\ln T}{d\ln r}\right\} r$$

- The temperature gradient $T(r)$ can be determined from the X-ray spectrum (or often the cluster is assumed to be isothermal).
- Emissivity depends on density squared, so the density gradient can be determined from the X-ray brightness.
- Note that one only measures the projected surface brightness of a cluster, not its 3-D brightness distribution. One must perform an "Abel integration" to infer the latter from the former.

Aside: The Sunyaev-Zel'dovich Effect

When microwave photons from the Big Bang pass through hot cluster gas, they scatter off the electrons and acquire energy in the process. (This is inverse-Compton scattering.) The result is a deficit of microwave photons (< 0.01%) in the direction of the cluster.

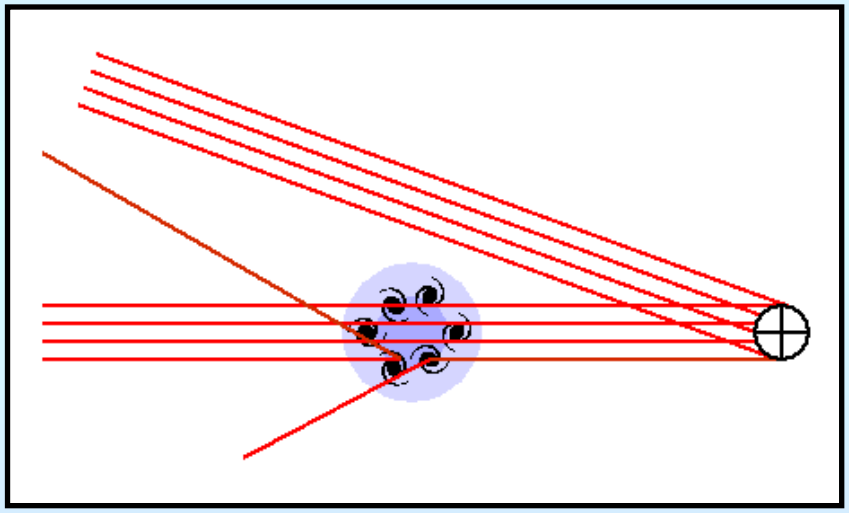

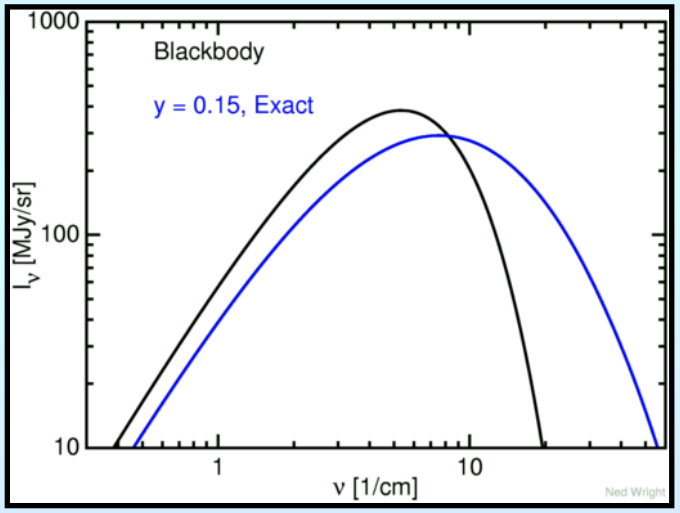

The amount of the deficit depends on the size of the cluster, through $y \propto \int n_e T_e \, dl$. Since one can observe the angular size of the cluster (and the X-ray luminosity depends on $L_x \propto \int n_e^2 \Lambda(T) \, dl$), a comparison of the two yields an independent measure of distance.

Gravitational Lenses

Any mass will cause light to deflect, with the angle of deflection (the Einstein angle) being

$$\alpha = \frac{4GM}{\xi c^2}$$

where ξ is the initial impact parameter, and M is the mass enclosed in the projected radius. (Note that this is twice the geometric angle.)

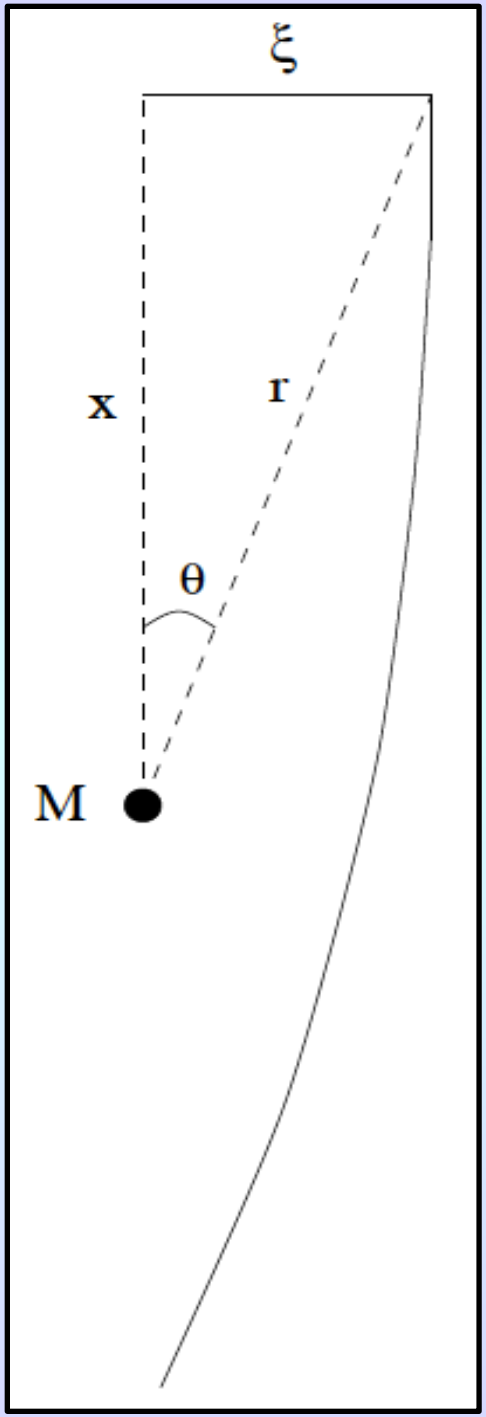

Gravitational Lenses

Any mass will cause light to deflect, with the angle of deflection (the Einstein angle) being

$$\alpha = \frac{4GM}{\xi c^2}$$

where ξ is the initial impact parameter, and M is the mass enclosed in the projected radius. (Note that this is twice the geometric angle.)

With respect to the lens, the relation between the true angular position of the source, β, and the observed position, θ, is given by

$$\beta = \theta - \frac{\alpha_0}{\theta} \quad \text{where} \quad \alpha_0 = \left(\frac{4GM}{c^2} \frac{D_{ds}}{D_d D_s} \right)^{1/2}$$

where D_d is the distance to the lens, D_s is the distance to the source, and D_{ds} is the distance from the lens to the source. The value α_0 is called the Einstein radius.

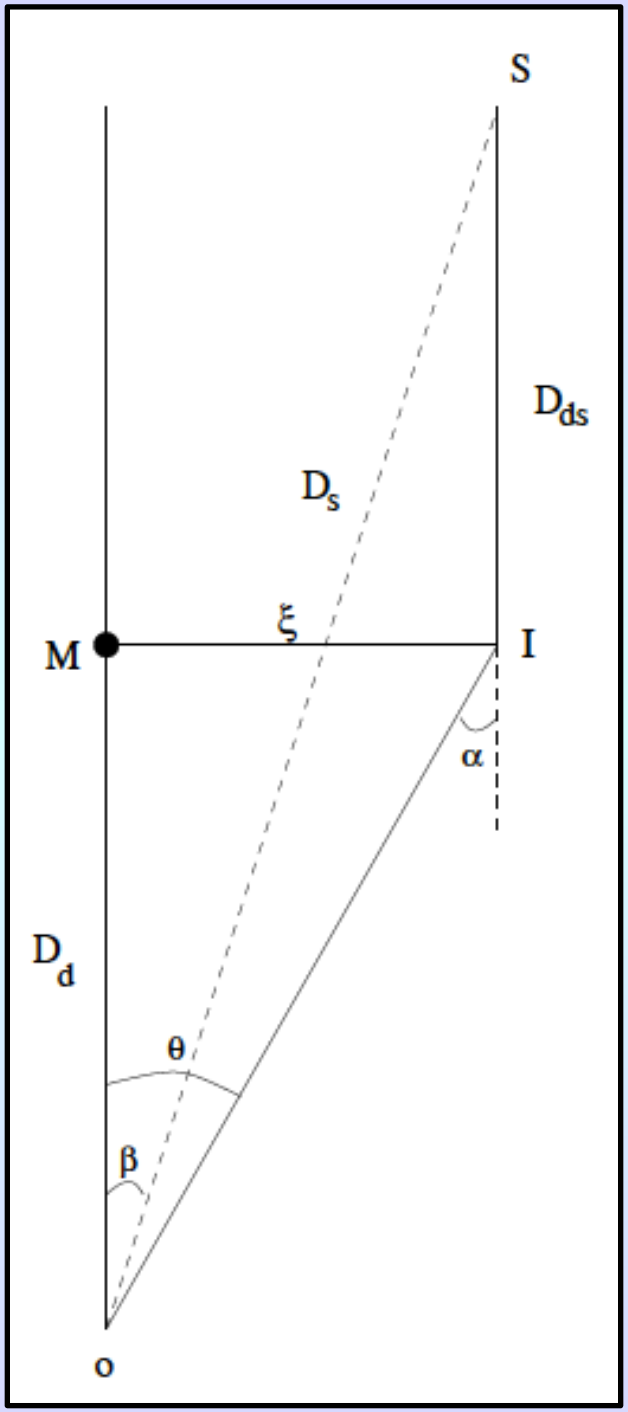

Gravitational Lens Magnifications

The equation relating β to θ is quadradic: $\beta = \theta - \frac{\alpha_0}{\theta} \Rightarrow \theta^2 - \beta\theta - \alpha_0 = 0$

The solution is $\theta = \frac{1}{2}\left(\beta \pm \sqrt{4\alpha_0^2 + \beta^2}\right)$

Without the lens, light falls into an area $dA = \beta\, d\phi\, d\beta$

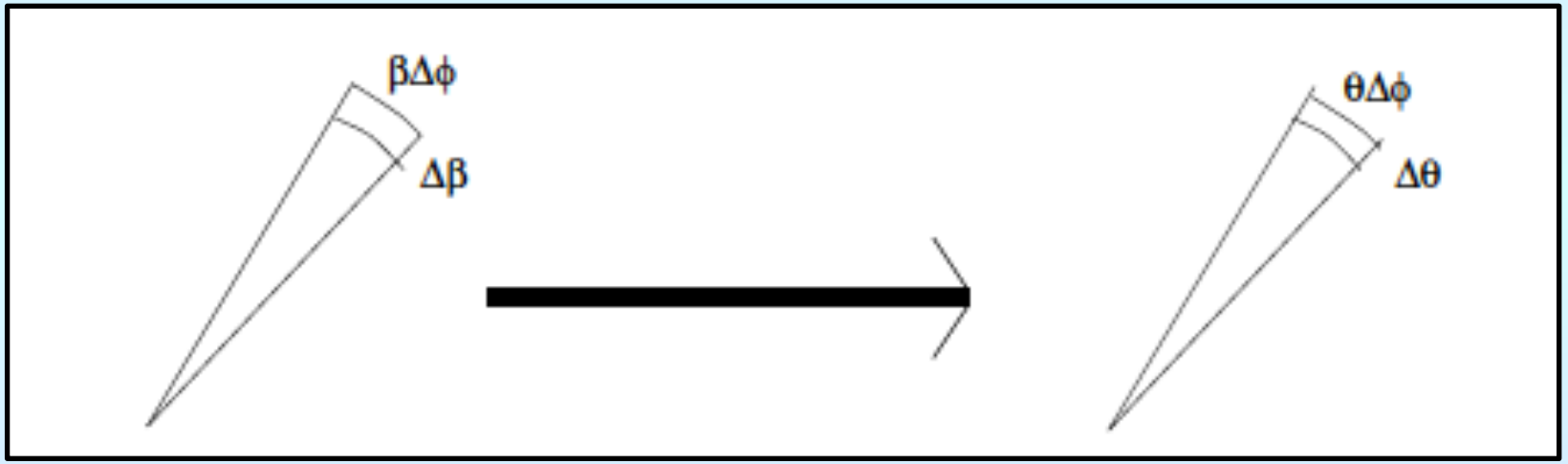

With the lens, this same light is focused into $dA' = \theta\, d\phi\, d\theta$. The magnification is therefore the ratio of the two areas,

$$\frac{d\theta}{d\beta} = \frac{1}{2}\left(1 \pm \frac{\beta}{\sqrt{4\alpha_0^2 + \beta^2}}\right) \quad \Rightarrow \quad \mu = \frac{1}{4}\left\{\frac{\beta}{\sqrt{4\alpha_0^2 + \beta^2}} + \frac{\sqrt{4\alpha_0^2 + \beta^2}}{\beta} \pm 2\right\}$$

Gravitational Lens Magnification

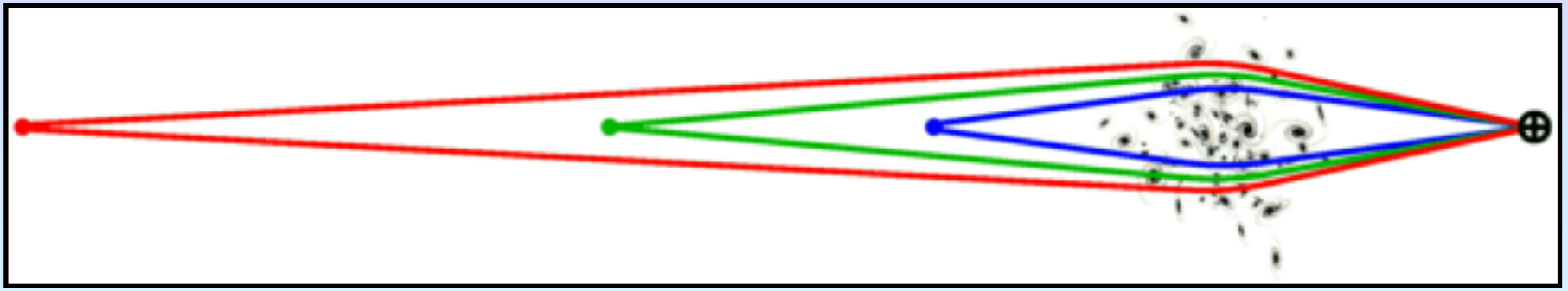

Background galaxies can be sheered and magnified into large arcs.
One can also get multiple images of background point sources.

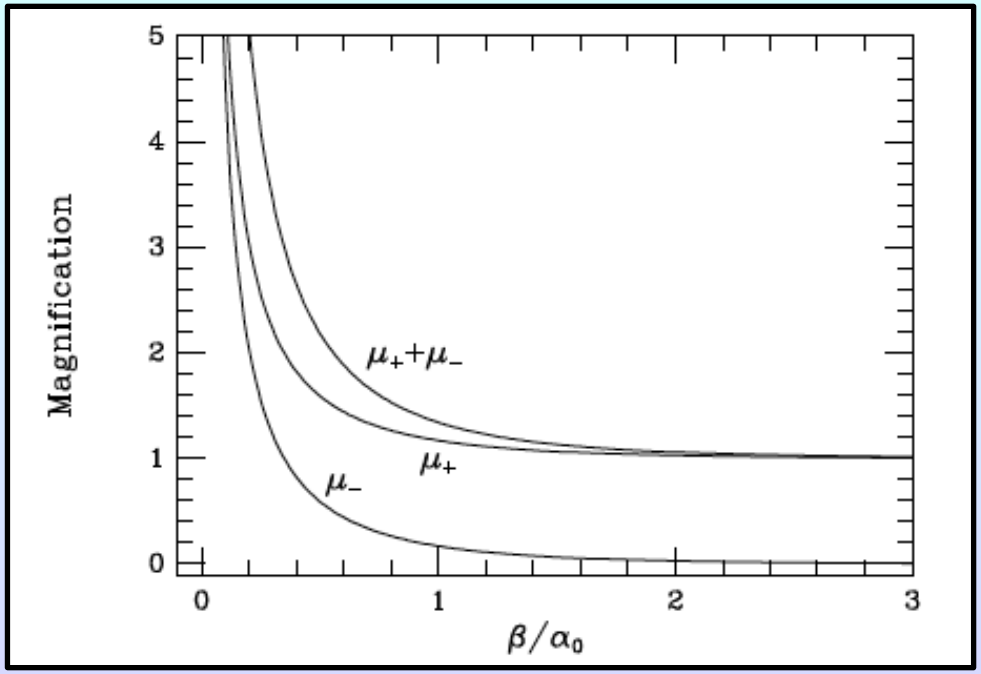

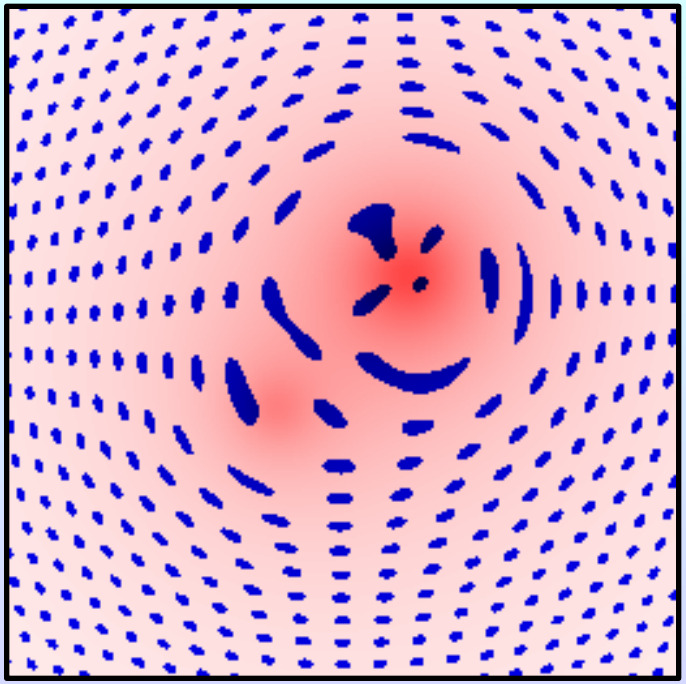

Gravitational Lens Regimes

There are several classes of gravitational lenses

- Microlens: The multiple gravitational lensed images cannot be resolved. Most often this occurs in the Galaxy (or LMC), when a foreground star (or planet) magnifies a background object.

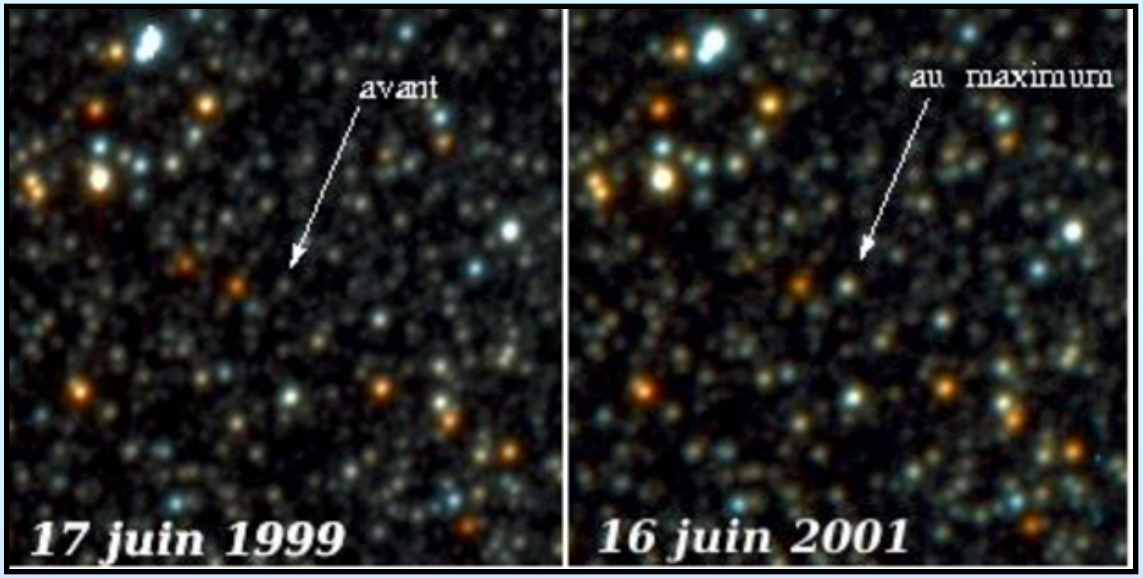

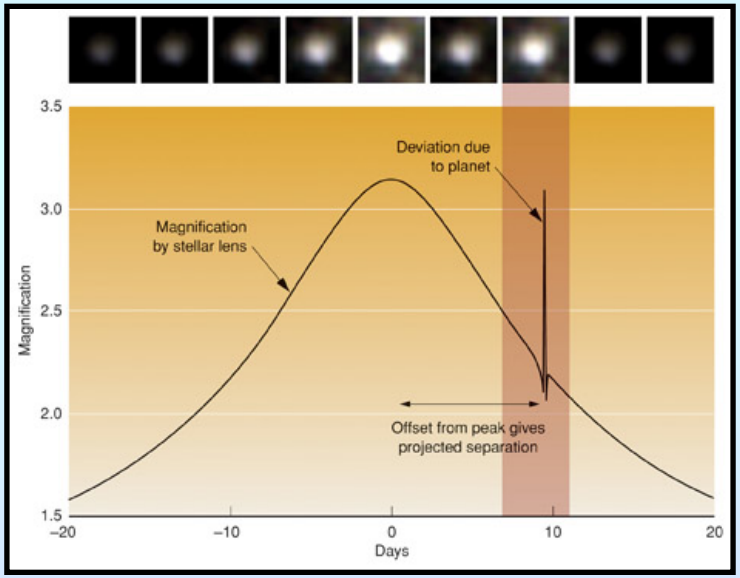

Gravitational Lens Regimes

There are several classes of gravitational lenses

- Microlens: The multiple gravitational lensed images cannot be resolved. Most often this occurs in the Galaxy (or LMC), when a foreground star (or planet) magnifies a background object.
- Strong Lensing: One observes multiple images or long arcs.

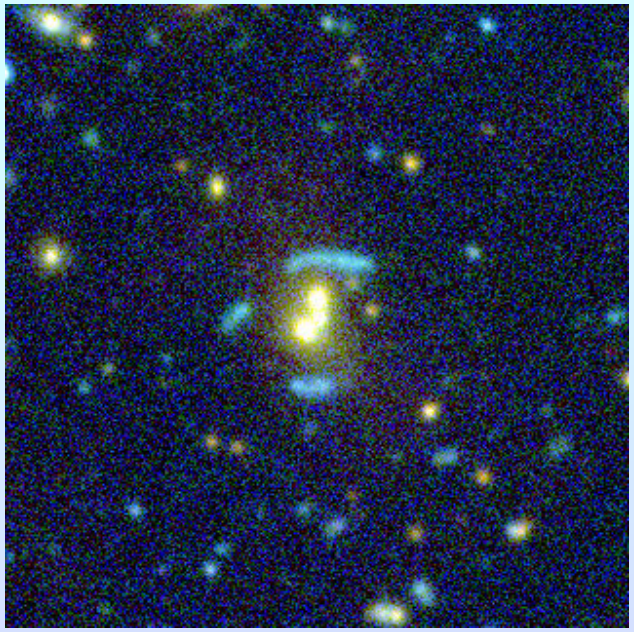

Gravitational Lens Regimes

There are several classes of gravitational lenses

- Microlens: The multiple gravitational lensed images cannot be resolved. Most often this occurs in the Galaxy (or LMC), when a foreground star (or planet) magnifies a background object.
- Strong Lensing: One observes multiple images or long arcs.

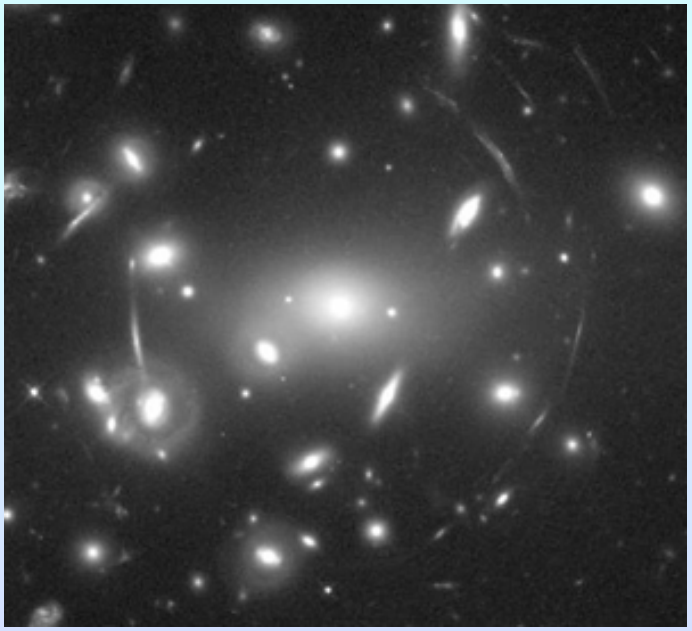

Gravitational Lens Regimes

There are several classes of gravitational lenses

- Microlens: The multiple gravitational lensed images cannot be resolved. Most often this occurs in the Galaxy (or LMC), when a foreground star (or planet) magnifies a background object.
- Strong Lensing: One observes multiple images or long arcs.
- Weak Lensing: The gravitational lens affect is not obvious, but statistically speaking, the shapes of the galaxies are distorted. (In other words, their elongations are not randomly distributed.)

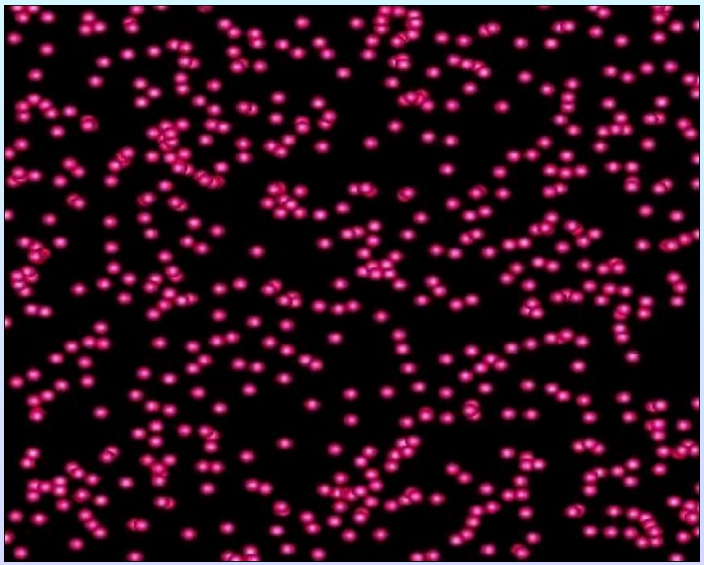

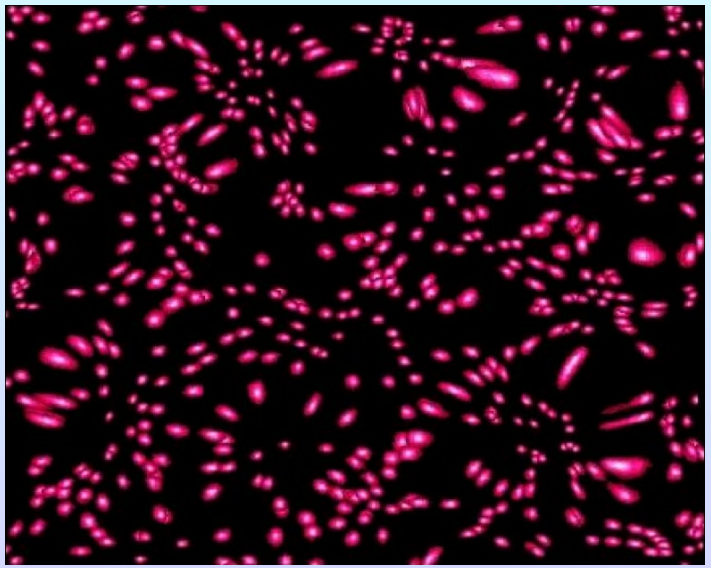

Gravitational Lens Regimes

There are several classes of gravitational lenses

- Microlens: The multiple gravitational lensed images cannot be resolved. Most often this occurs in the Galaxy (or LMC), when a foreground star (or planet) magnifies a background object.
- Strong Lensing: One observes multiple images or long arcs.
- Weak Lensing: The gravitational lens affect is not obvious, but statistically speaking, the shapes of the galaxies are distorted. (In other words, their elongations are not randomly distributed.)

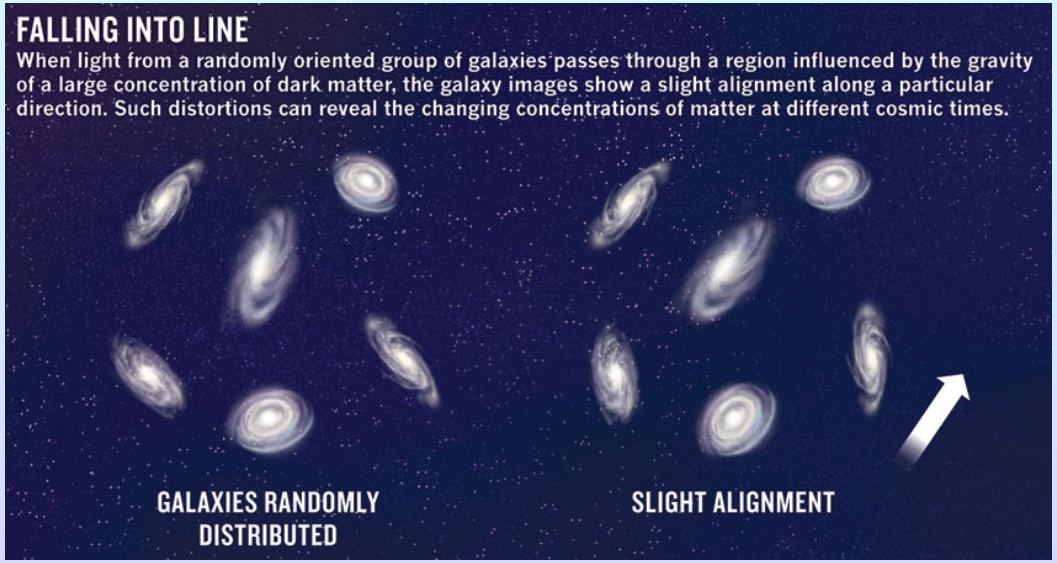

Gravitational Lenses Magnification

Each lens/arc provides a constraint on the lens. By carefully examining the shapes of distant galaxies, one can derive the mass distribution of the lens.

Gravitational Lenses Magnification

Each lens/arc provides a constraint on the lens. By carefully examining the shapes of distant galaxies, one can derive the mass distribution of the lens.